Investigating Novel Battery Cooling Strategies Using Phase-Change Materials Through Detailed 3D CFD Simulations

Kislaya Srivastava, Tristan Burton

Convergent Science Inc., Northville, MI 48167

CONVERGE CFD for Battery Simulations

- CONVERGE CFD software is well-suited for battery simulations of 3D coupled flow, heat transfer, and chemistry in complex geometries, with autonomous mesh generation to reduce total time-to-solution
- CONVERGE contains the SAGE detailed chemical kinetics solver, parallelized efficiently for fast run-times and adopted to model battery vent gas combustion and thermal runaway chemistry inside the solid
- Adaptive mesh refinement (AMR) automatically resolves the flow, diffusion of vent gas, flame front and thermal runaway front propagation at low computational expense
- Wide variety of other physics-based 3D modeling capabilities that have been utilized for battery simulations

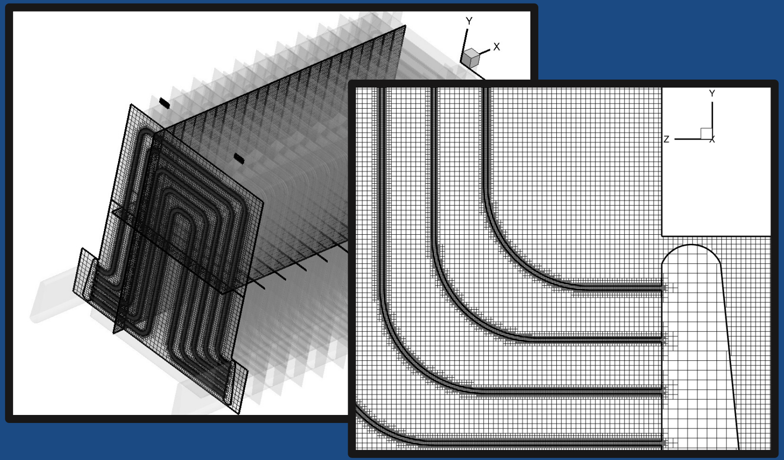

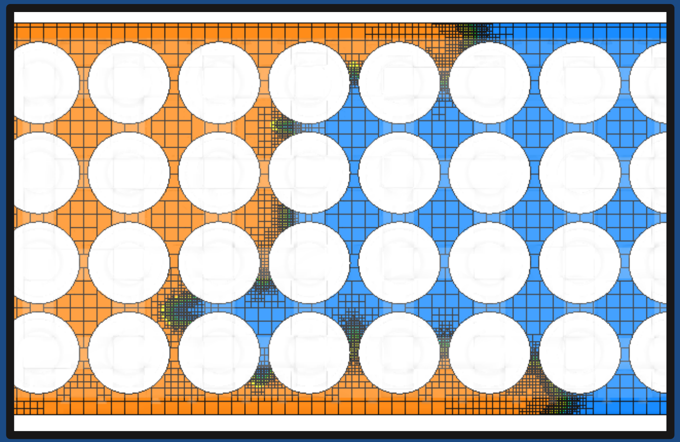

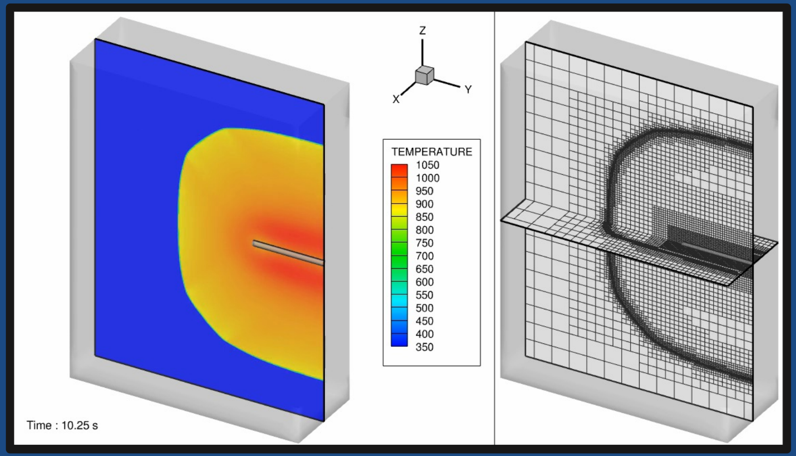

Thermal Runaway Propagation and Vent Gas Simulations

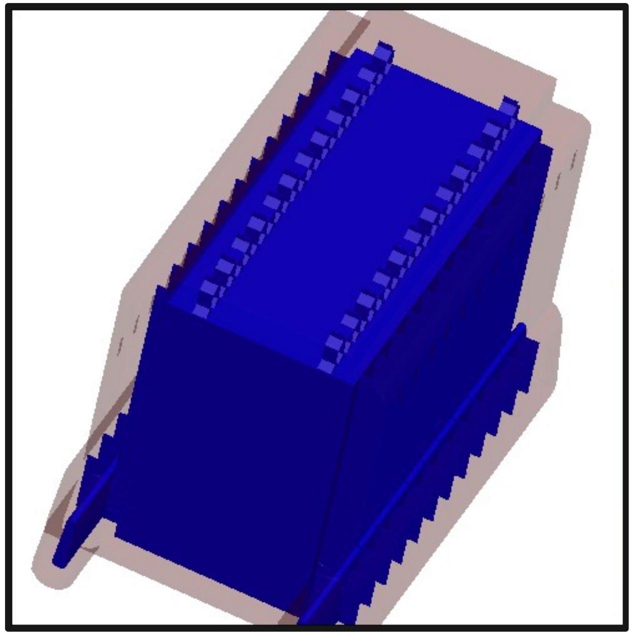

Coupled thermal runaway and vent gas modeling frameworks

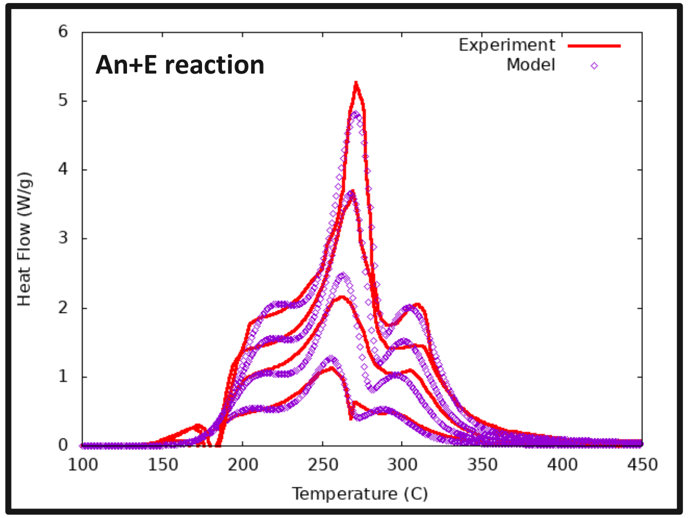

Thermal runaway mechanism fitting tools

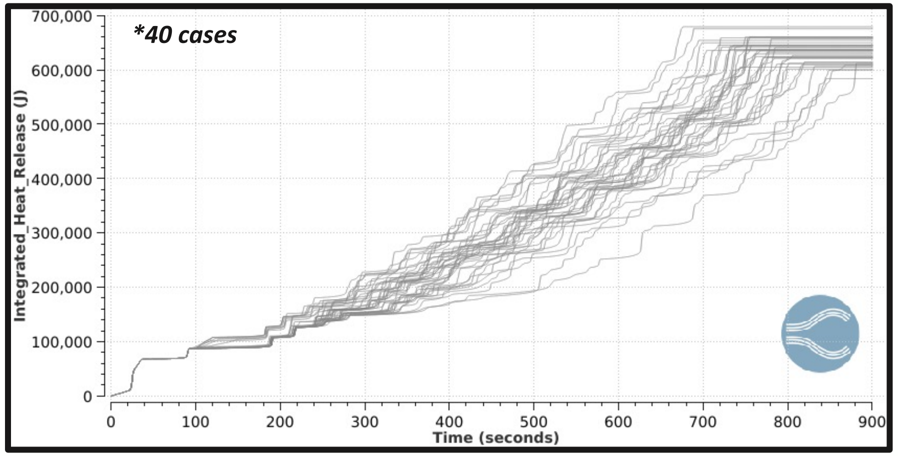

Statistical analysis of thermal runaway propagation in battery packs

Capturing Battery Thermal Runaway and Venting Phenomena using Detailed 3D CFD Solutions

Kislaya Srivastava et.al,

2022 NASA Aerospace Battery Workshop

Phase-Change Materials : An Overview

- Heat storage device : Absorbs heat during melting, releases heat during solidification
  - Temperature regulators
- Passive cooling approach : Lightweight, compact, efficient, consistent, sustainable
- Versatile : Variety of PCMs with broad spectrum of transition temperatures
  - Selection based on optimal battery operating temperature

- Drawbacks : Low conductivity, possible leakages, possible structural failures at high temperatures
- Conductivity/heat transfer can be enhanced using fins

PCMs with CFD : Solidification and Melting Model

- Solid-liquid phase change modeled using the enthalpy-porosity method
- Porosity of PCM :
  - 1 : Solid, *T < T_solidus*
  - 0: Liquid, *T > T_liquidus*
  - Between 0 and 1 : Mushy zone with liquid volume fraction, *T_solidus < T < T_liquidus*
- Liquid flow modeled as laminar and incompressible Newtonian fluid
- Boussinesq approximation to model buoyancy effect
- Transient 3D conjugate heat transfer simulations of PCM battery cooling investigated

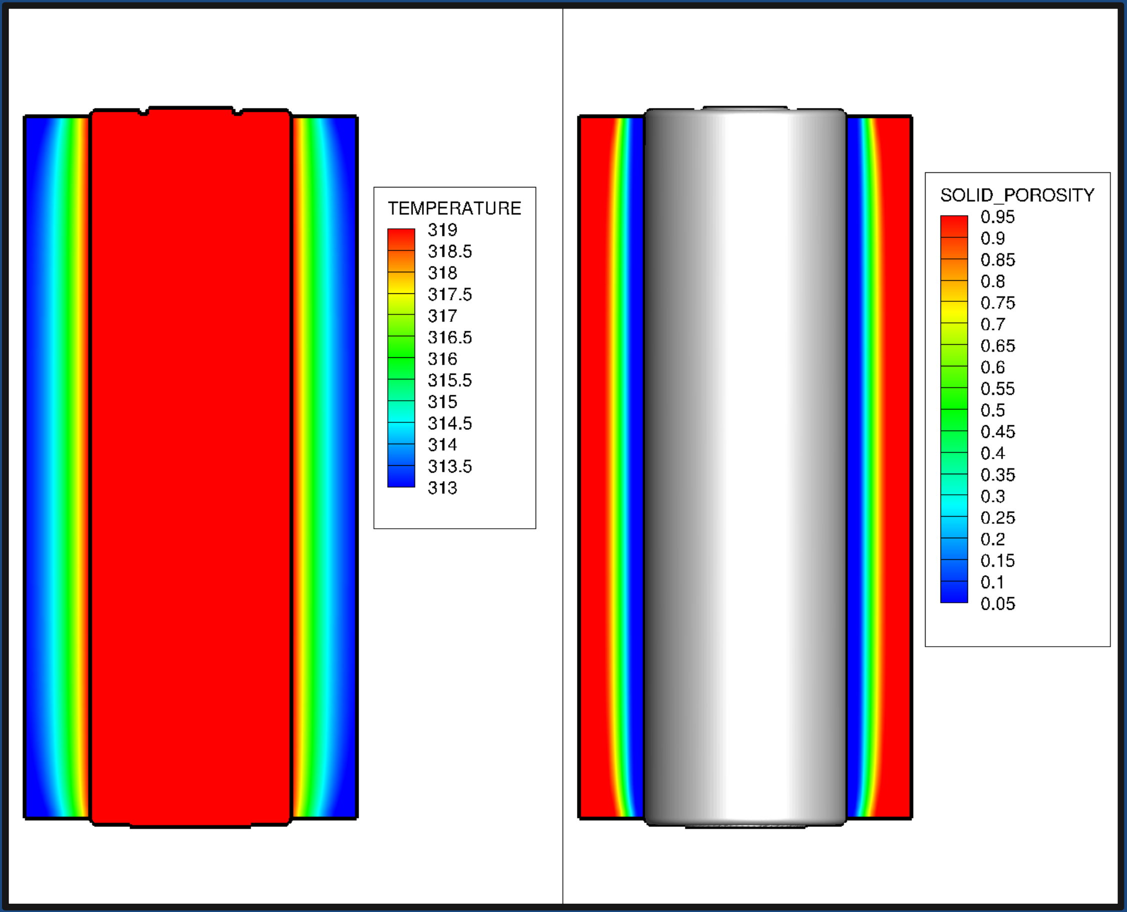

PCM : Paraffin wax (melting range : 314-317K)

Battery Equivalent Circuit Model

- Lumped-parameter model for electrothermal response
  - Simplistic and computationally inexpensive, empirical
  - Lin. et. al., “ *A lumped-parameter electro-thermal model for cylindrical batteries*”
- Represent battery as an electrical network and calculate heat source based on current (charging or discharging)
  - Inputs : battery capacity, initial SOC, current profile, 1D/2D data tables

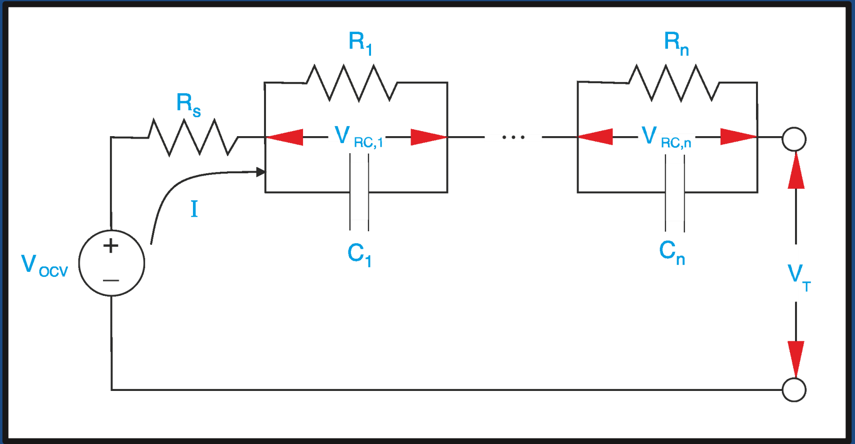

Terminal voltage:

$$V_T = V_{OCV} - IR_S - \sum_{i=1}^{n} V_{RC,i}$$

$$\frac{dV_{RC,i}}{dt} = -\frac{1}{R_i C_i} V_{RC,i} + \frac{1}{C_i} I$$

$$\frac{dSOC}{dt} = -\frac{1}{C_{bat}} I$$

$$Q = I(V_{OCV} - V_T)$$

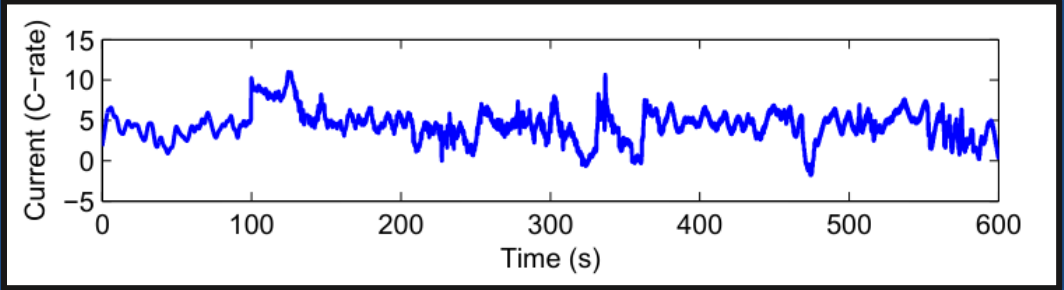

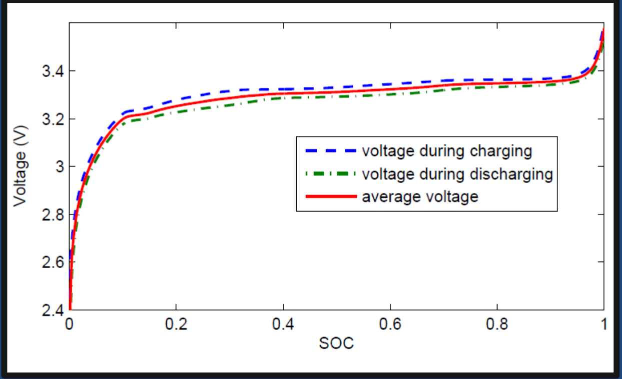

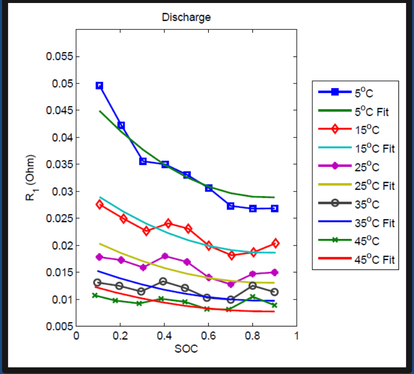

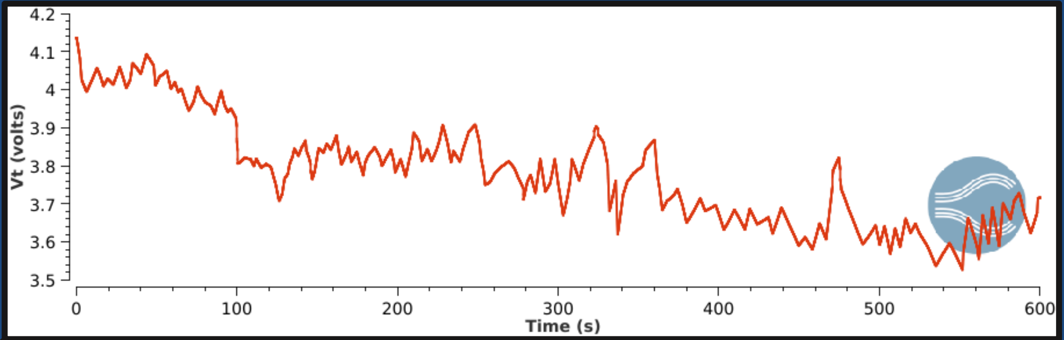

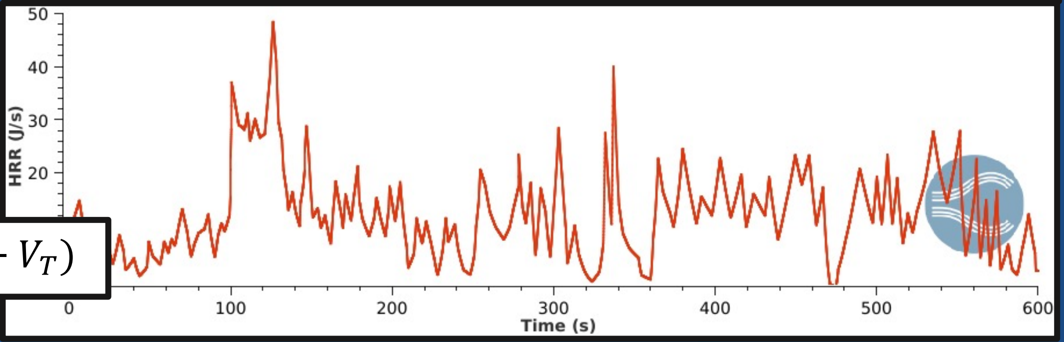

PCM Simulations : Results (1/2)

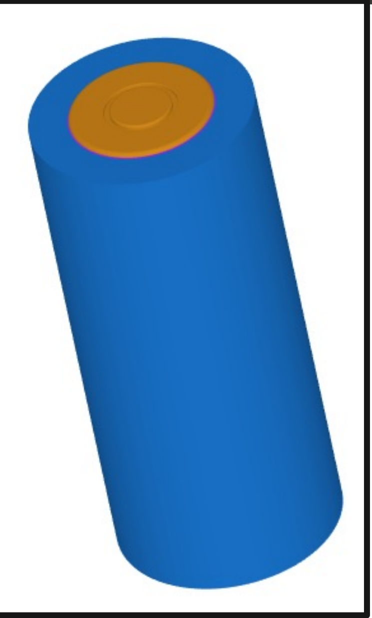

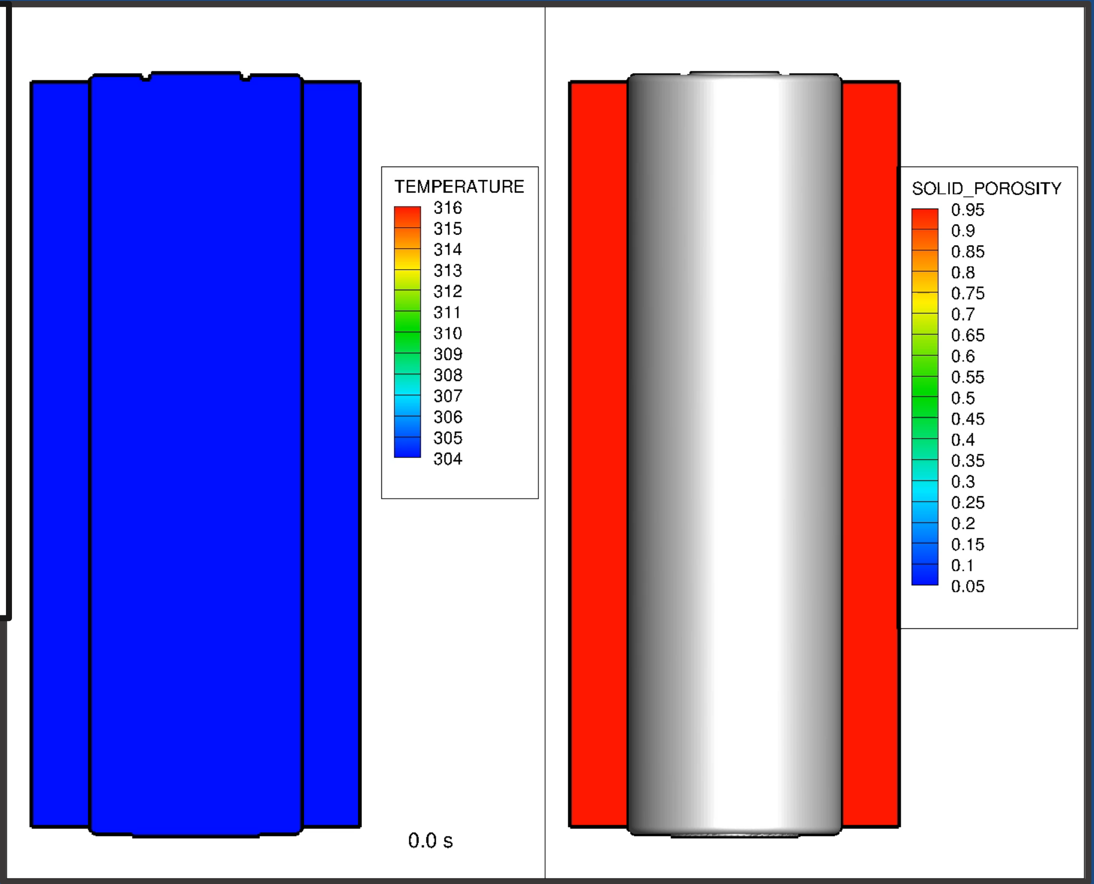

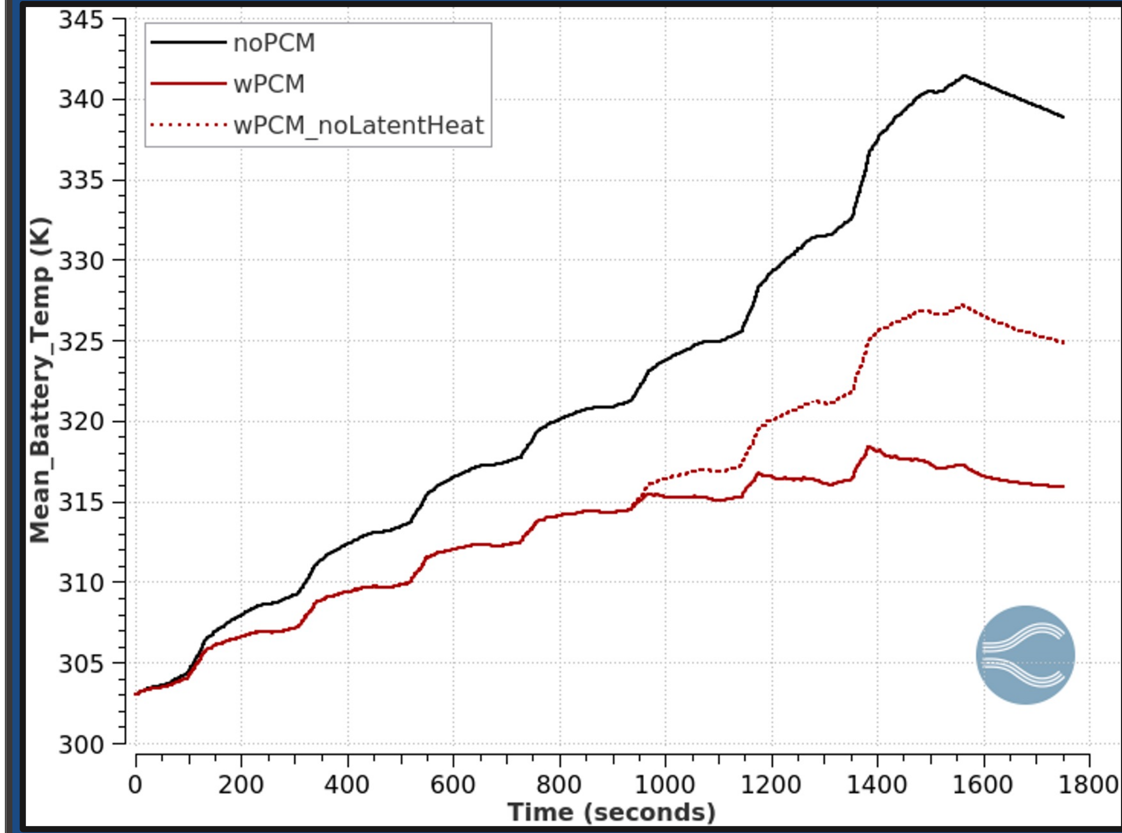

BEC for battery heat release under a low C-rate charge cycle
PCM : Paraffin wax (melting range : 314-317K)

PCM Simulations : Results (2/2)

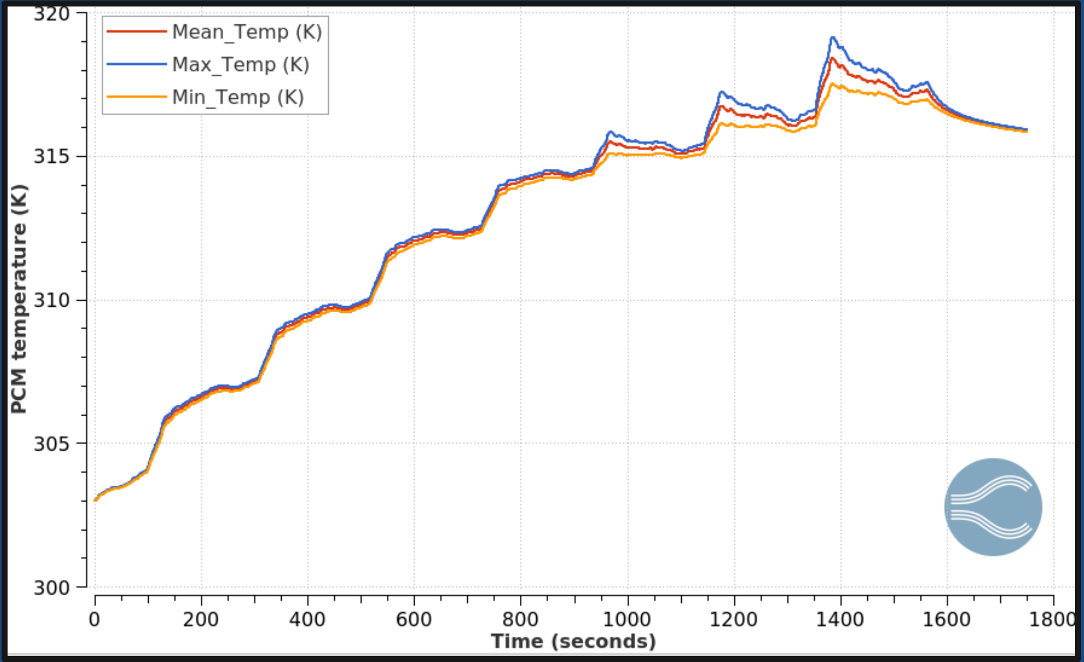

Temperatures within the PCM material

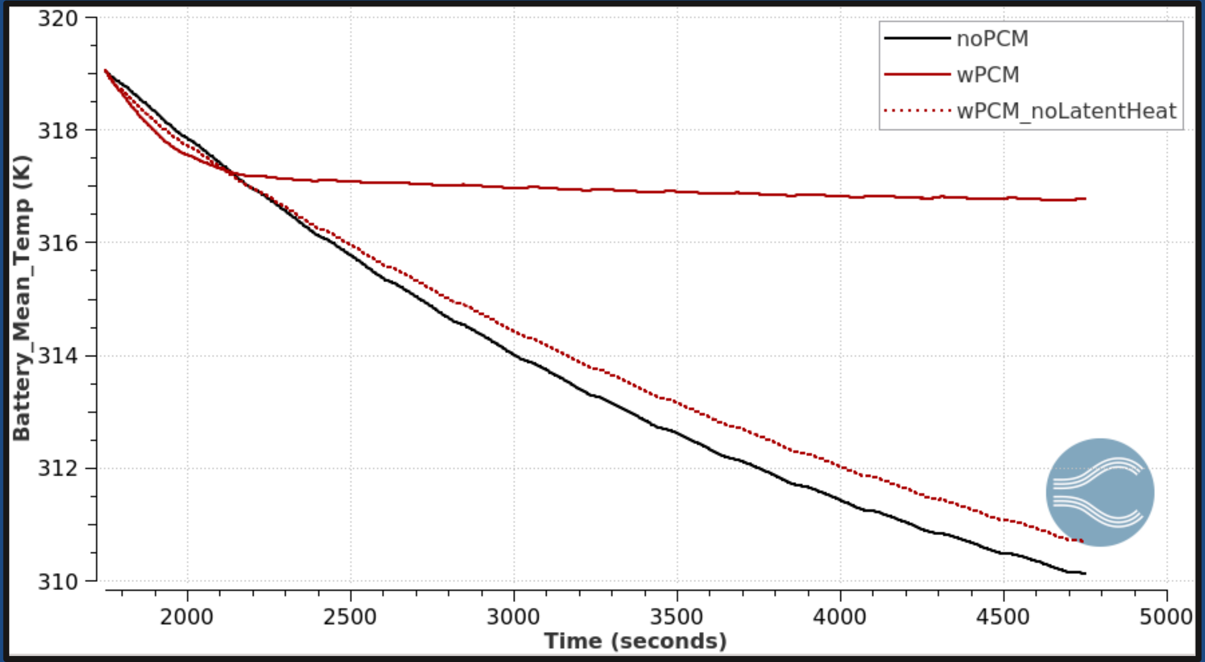

Temperature regulation (warming) during cooldown : Latent heat released during solidification

PCM Material Selection

	Paraffin	RT50	N-Eicosane	Lauric acid
Temp_liquidus (K)	317.15	324.15	310.50	321.35
Temp_solidus (K)	314.15	318.15	306.50	316.65
Specific Heat Capacity (K/Kg.K)	2000	2950	1926	2180
Latent heat capacity (J/kg)	255000	168000	248000	187210
Density (Kg/m3)	880	880	910	940
Conductivity (W/mK)	0.13	0.19	0.423	0.16

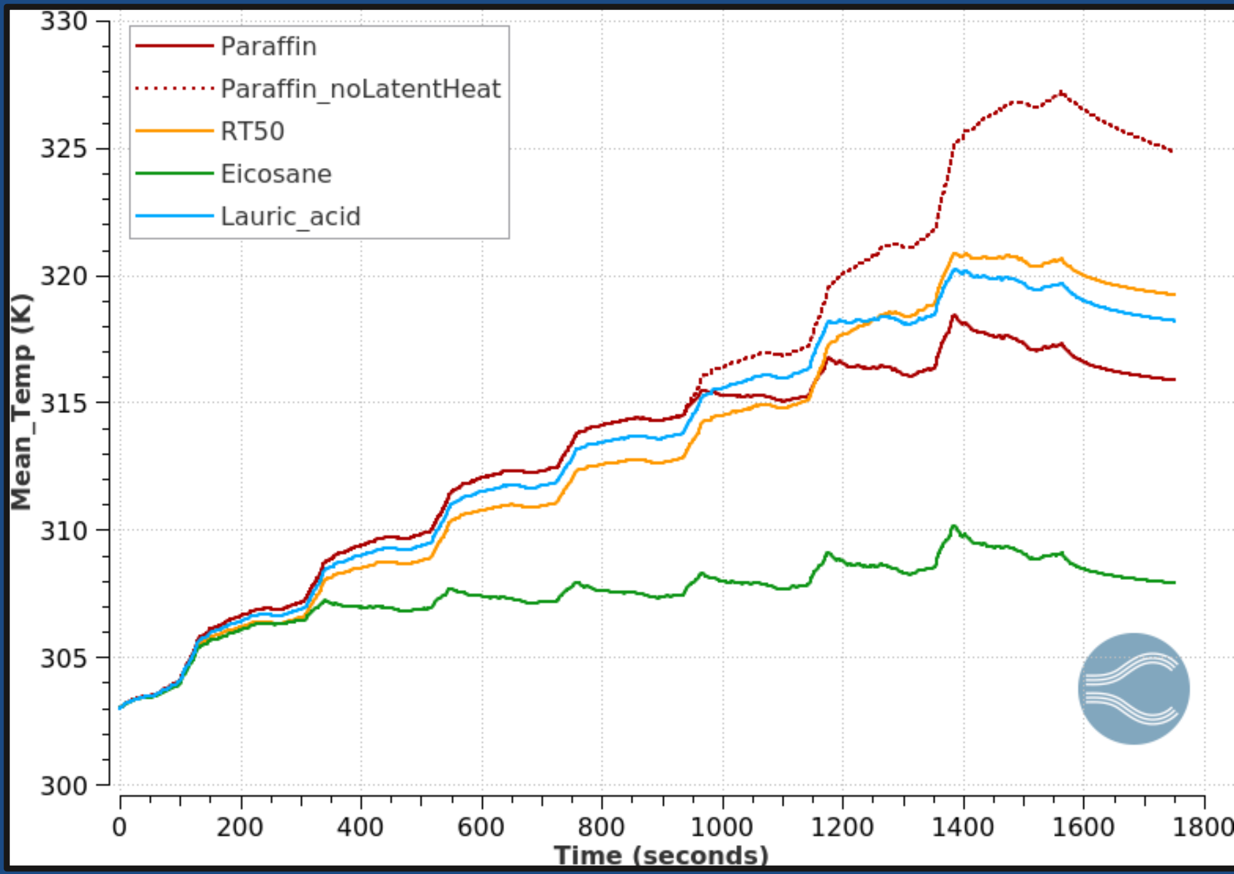

Addressing PCM Drawbacks : Low Conductivity

- Composites

	Conductivity (W/m.K)	Specific heat capacity (J/Kg.K)	Latent heat capacity (J/kg)	Temp liquidus (K)	Temp solidus (K)
RT44HC	0.21	2250	270000	317.15	314.15
CPCM	11.00	2500	107800	318.15	314.15

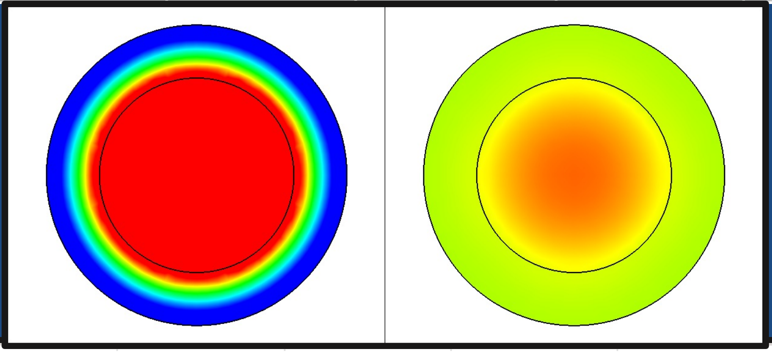

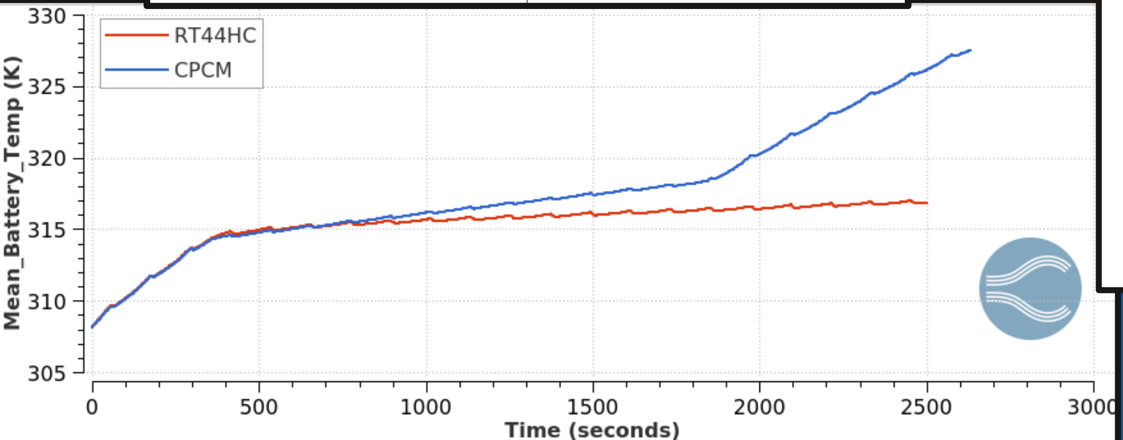

- Addition of fins

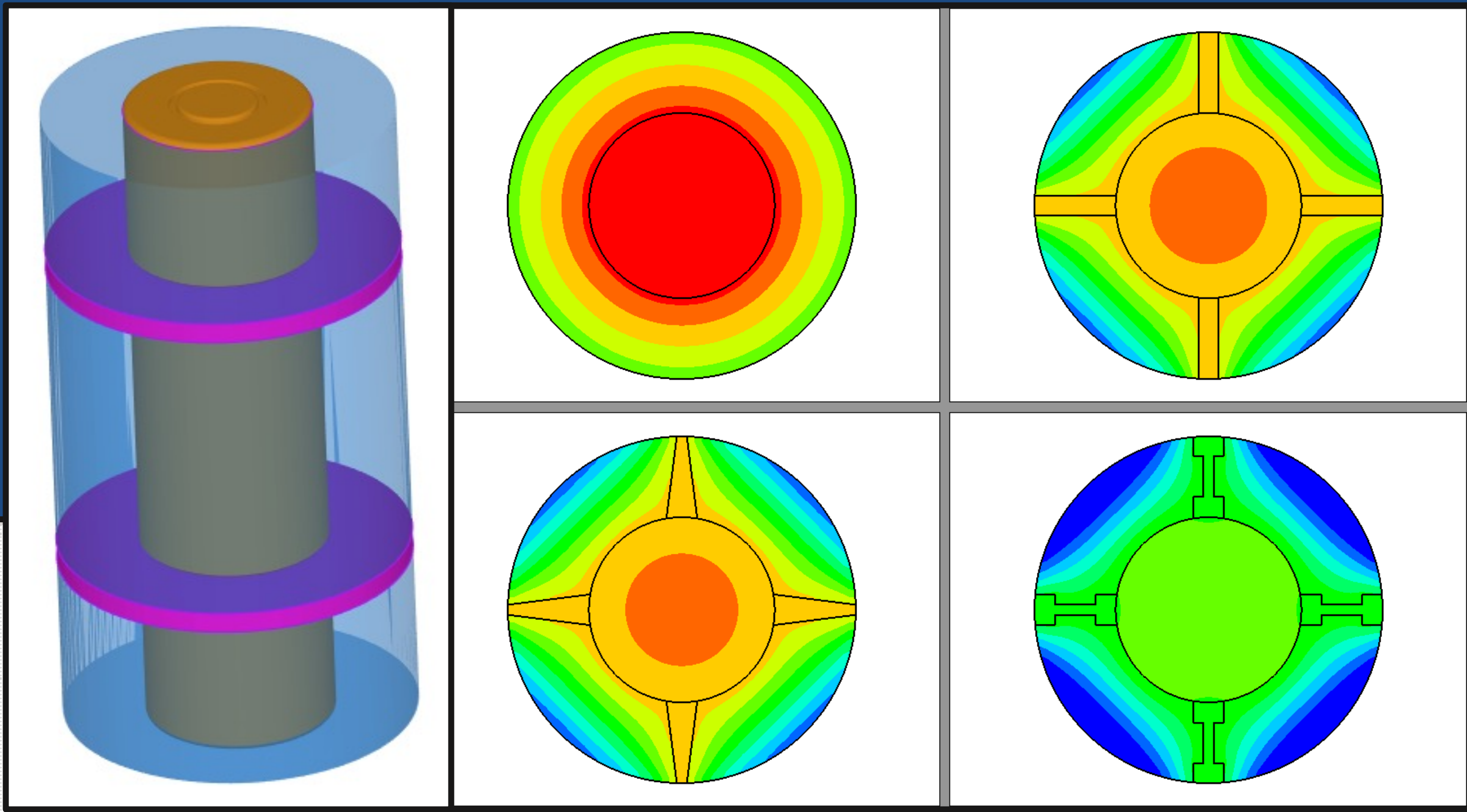

Fluid Dynamics Within PCMs

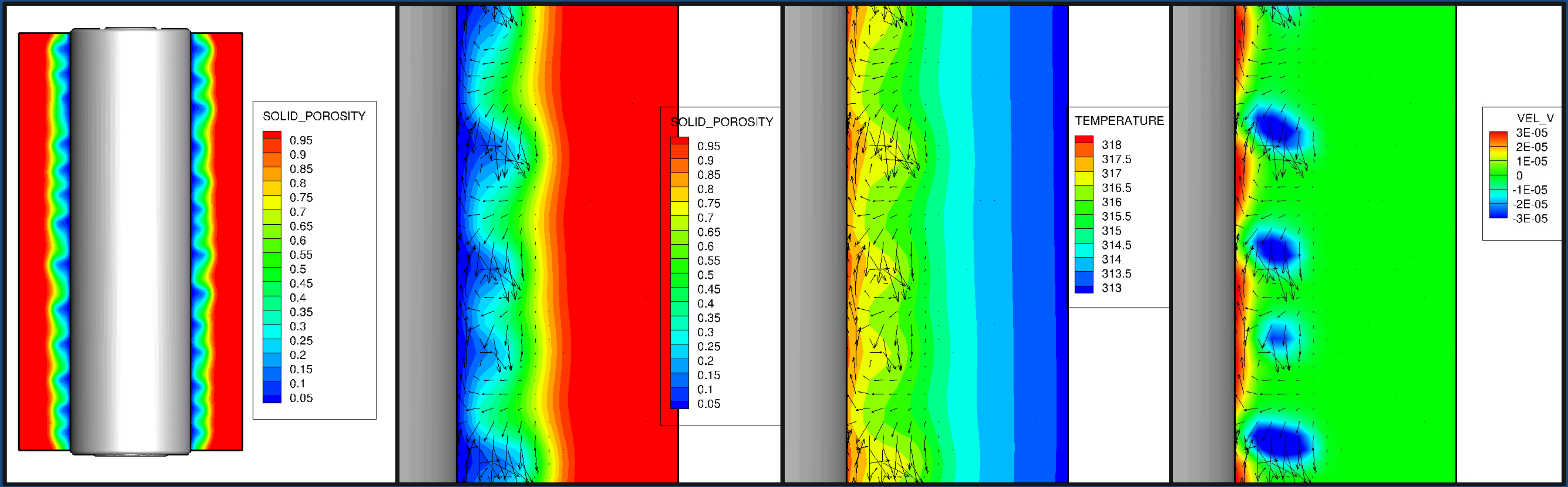

Fluid Dynamics Within PCMs : Natural Convection (1/2)

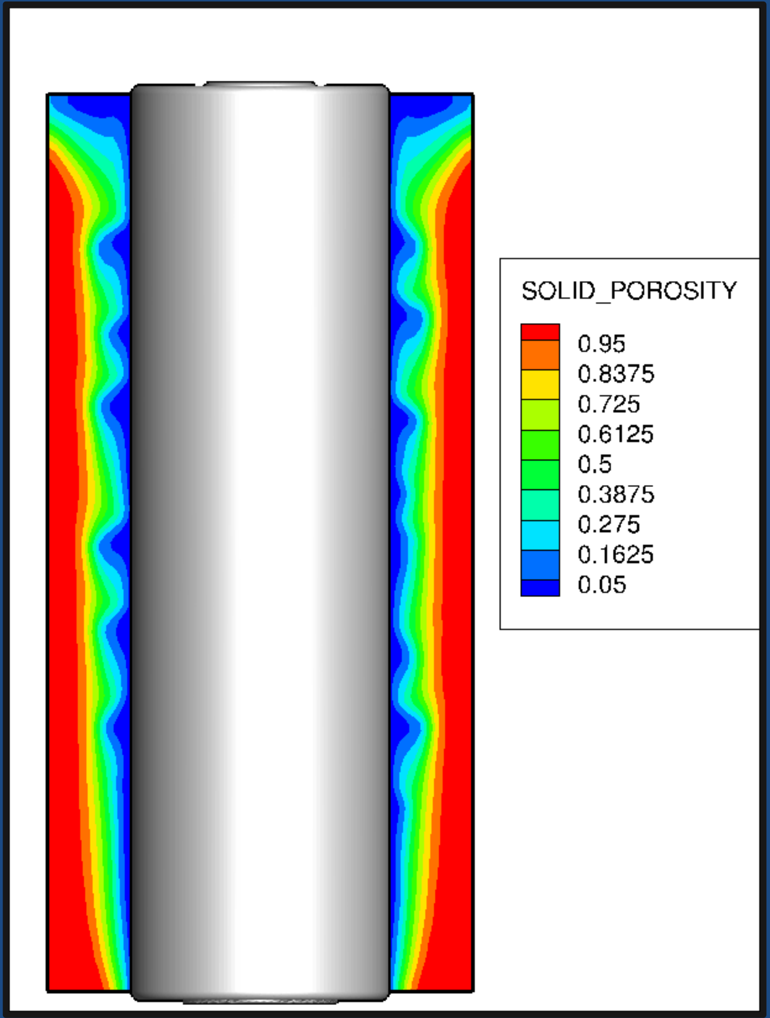

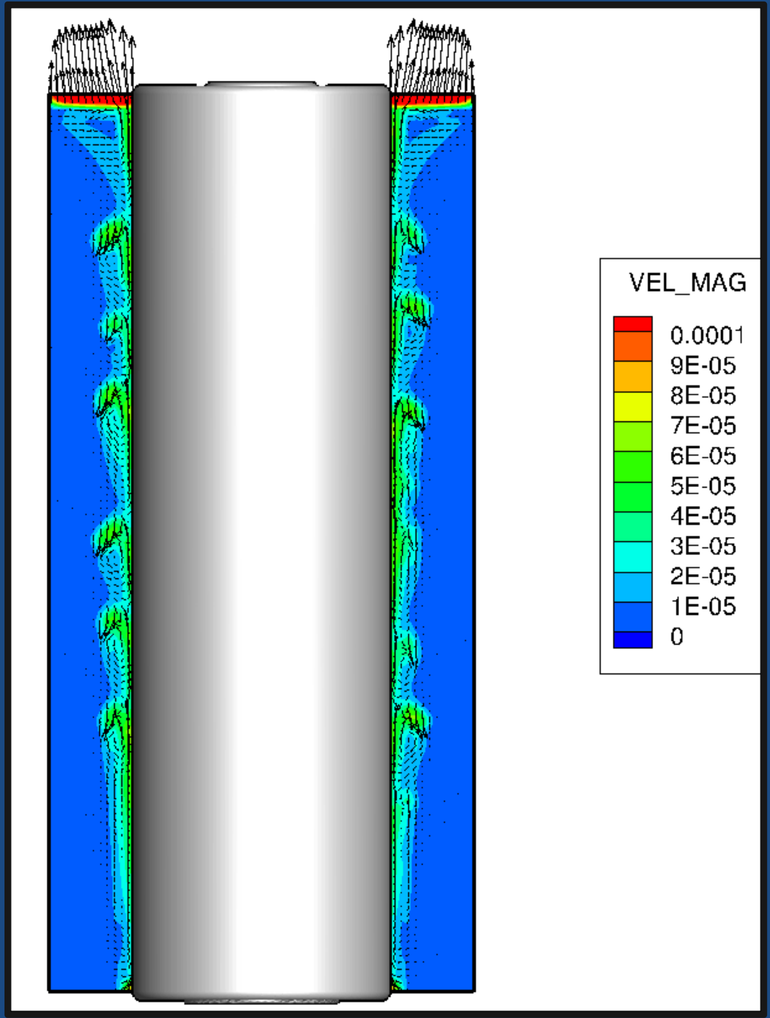

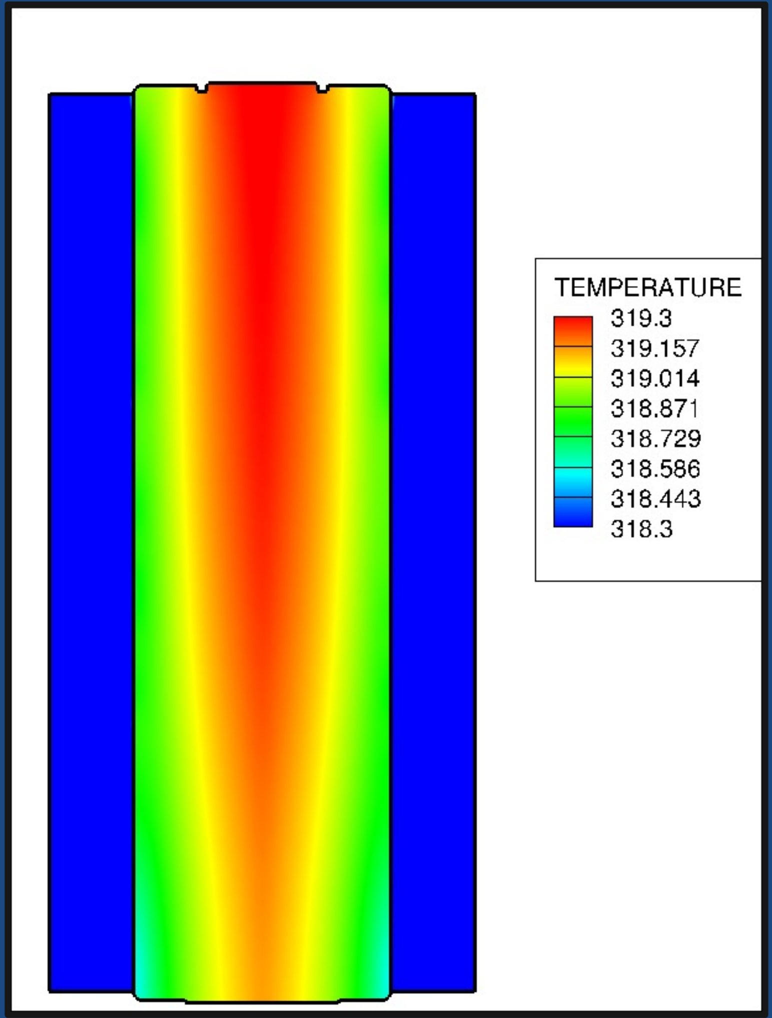

Fluid Dynamics Within PCMs : Natural Convection (2/2)

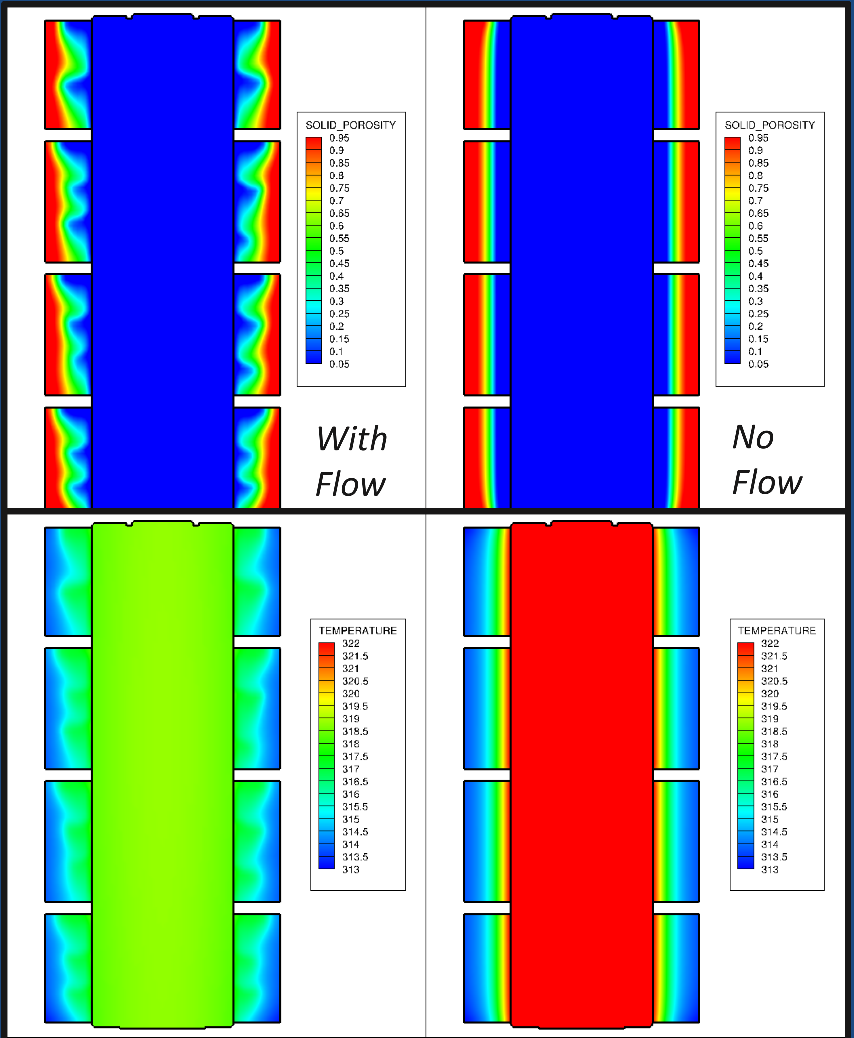

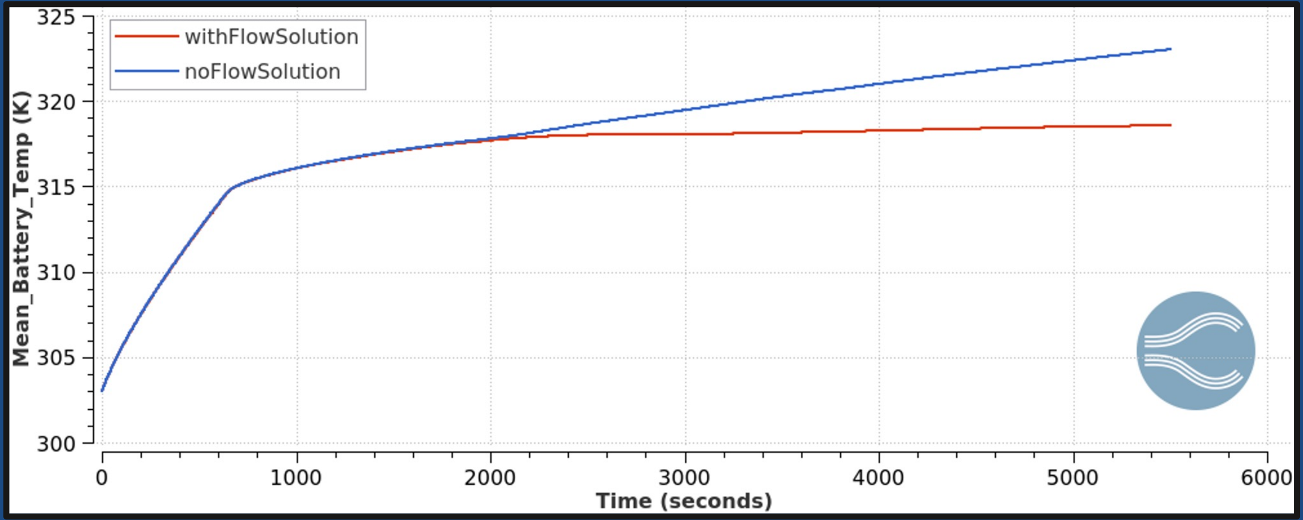

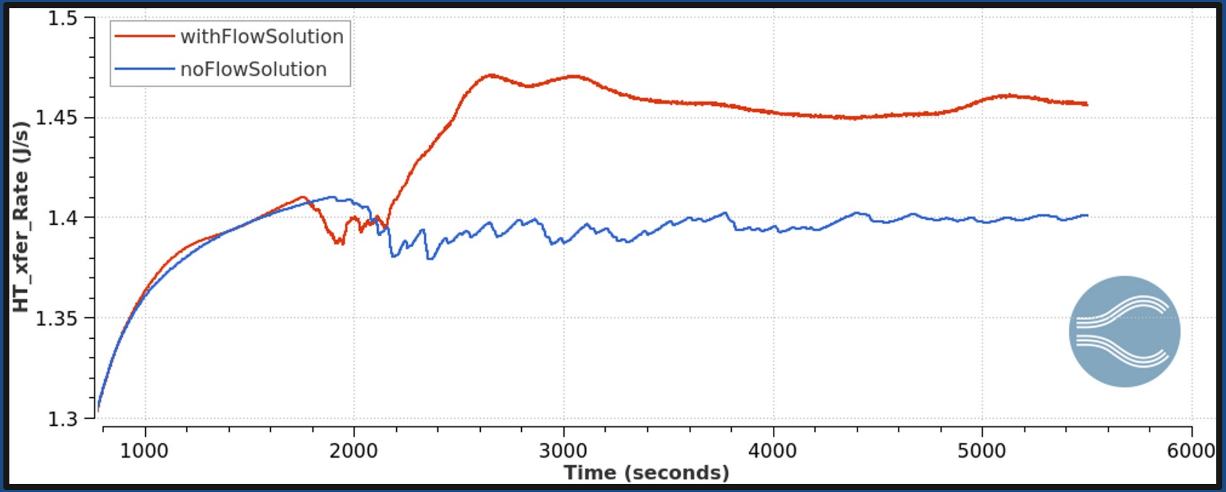

Fin Design Improvements : Helical Fin

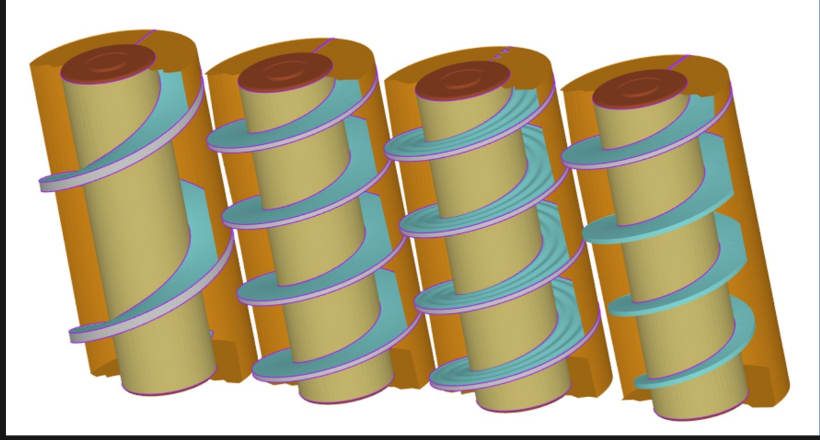

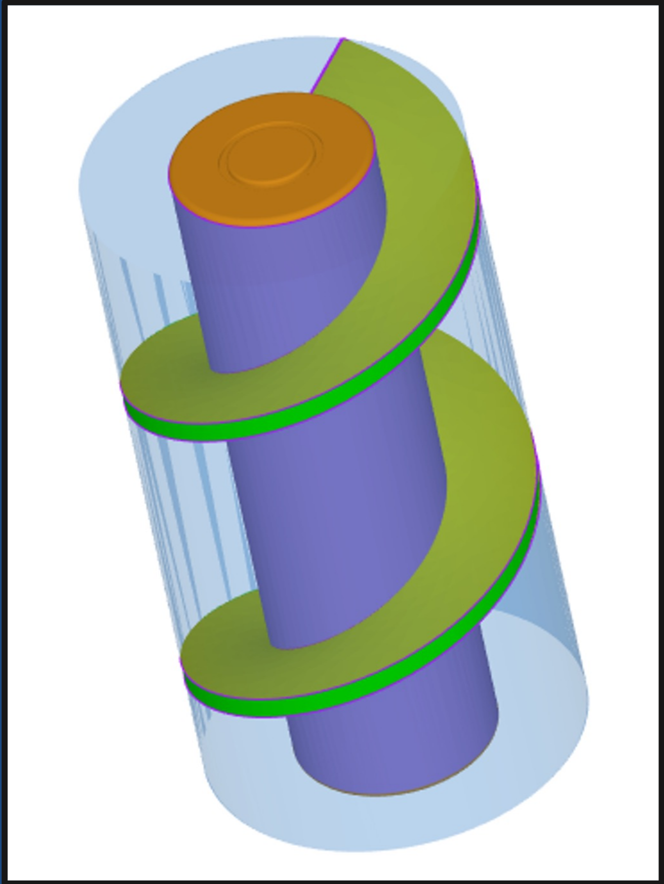

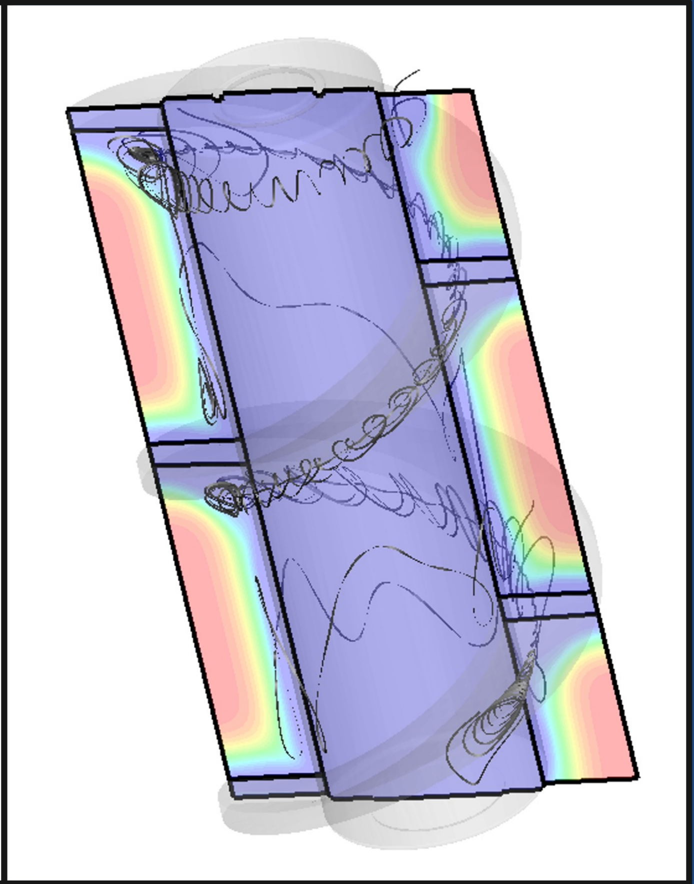

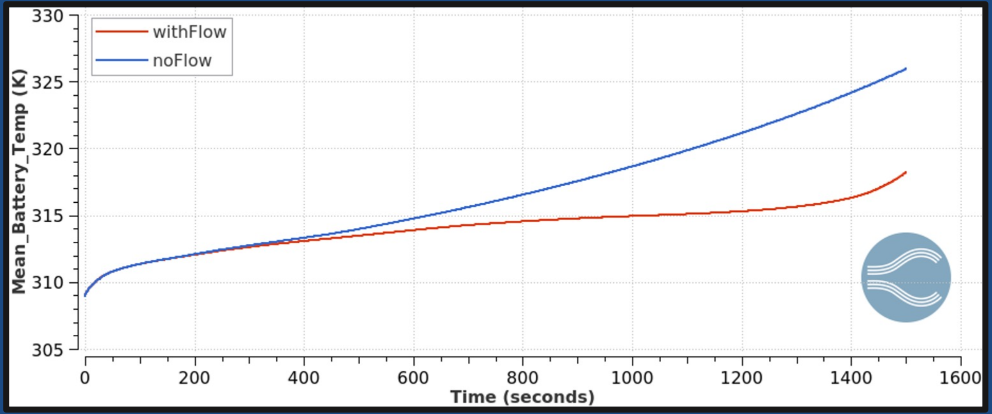

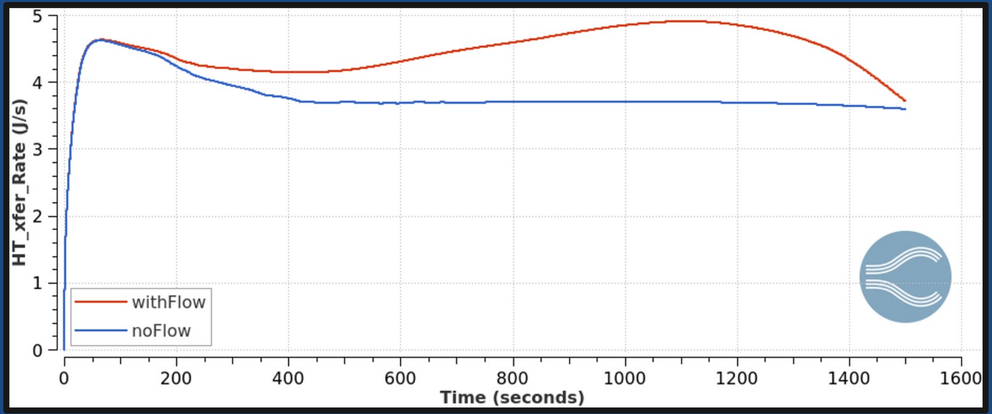

Fin Design Improvements : Double Helical Fin (1/2)

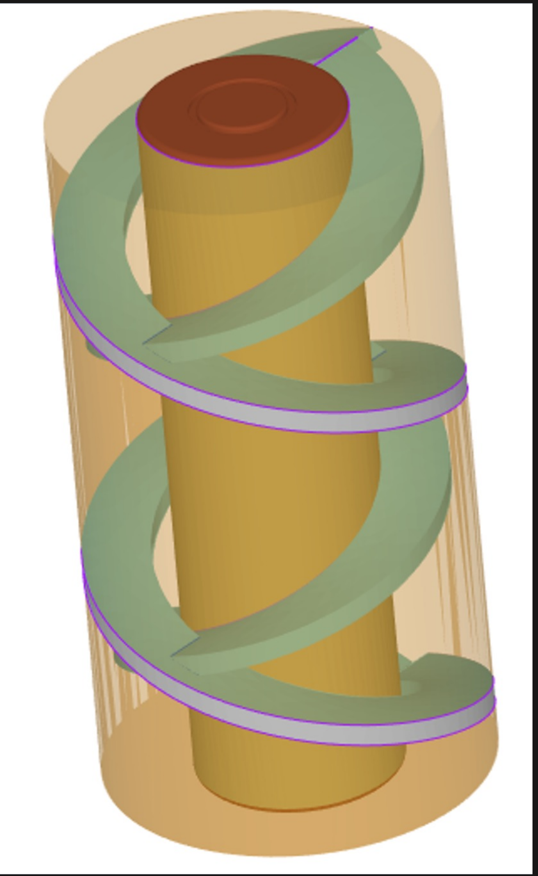

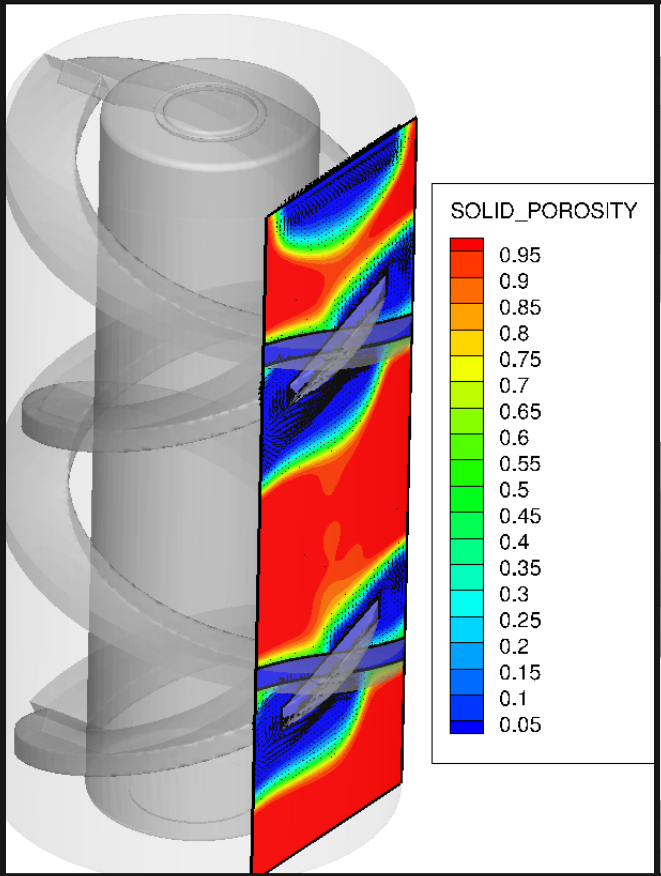

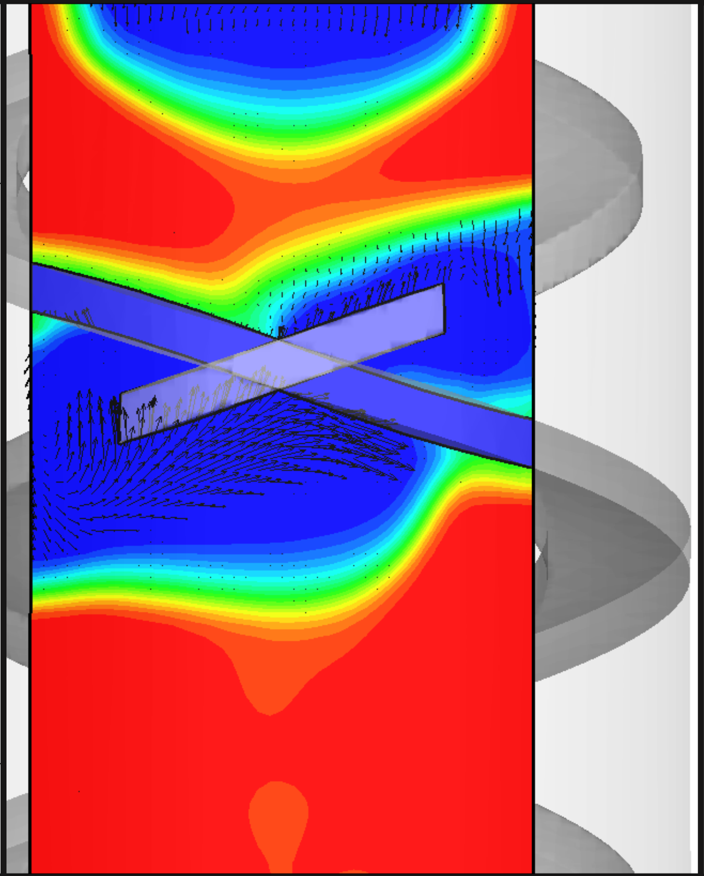

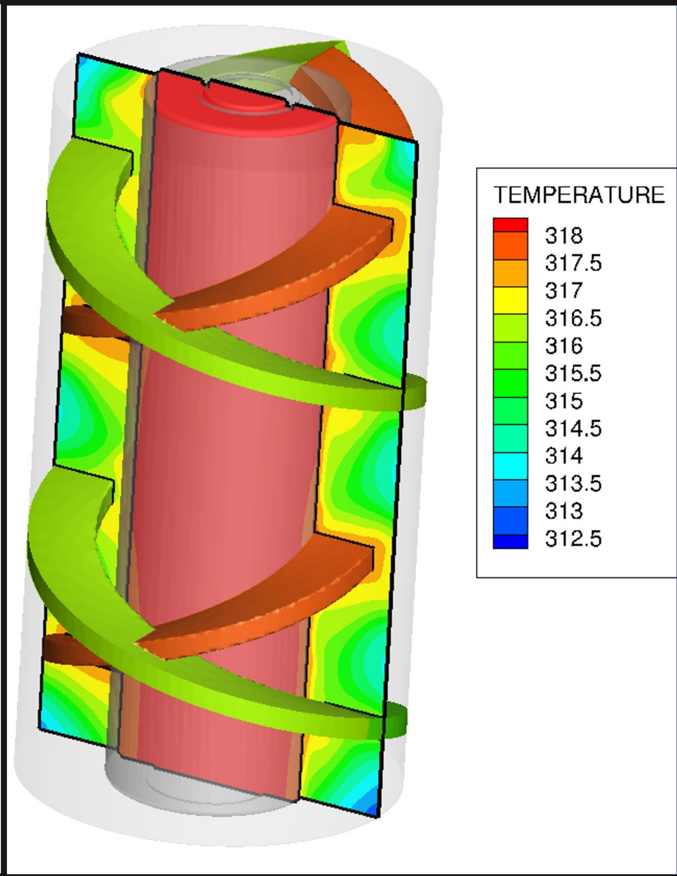

Fin Design Improvements : Double Helical Fin (2/2)

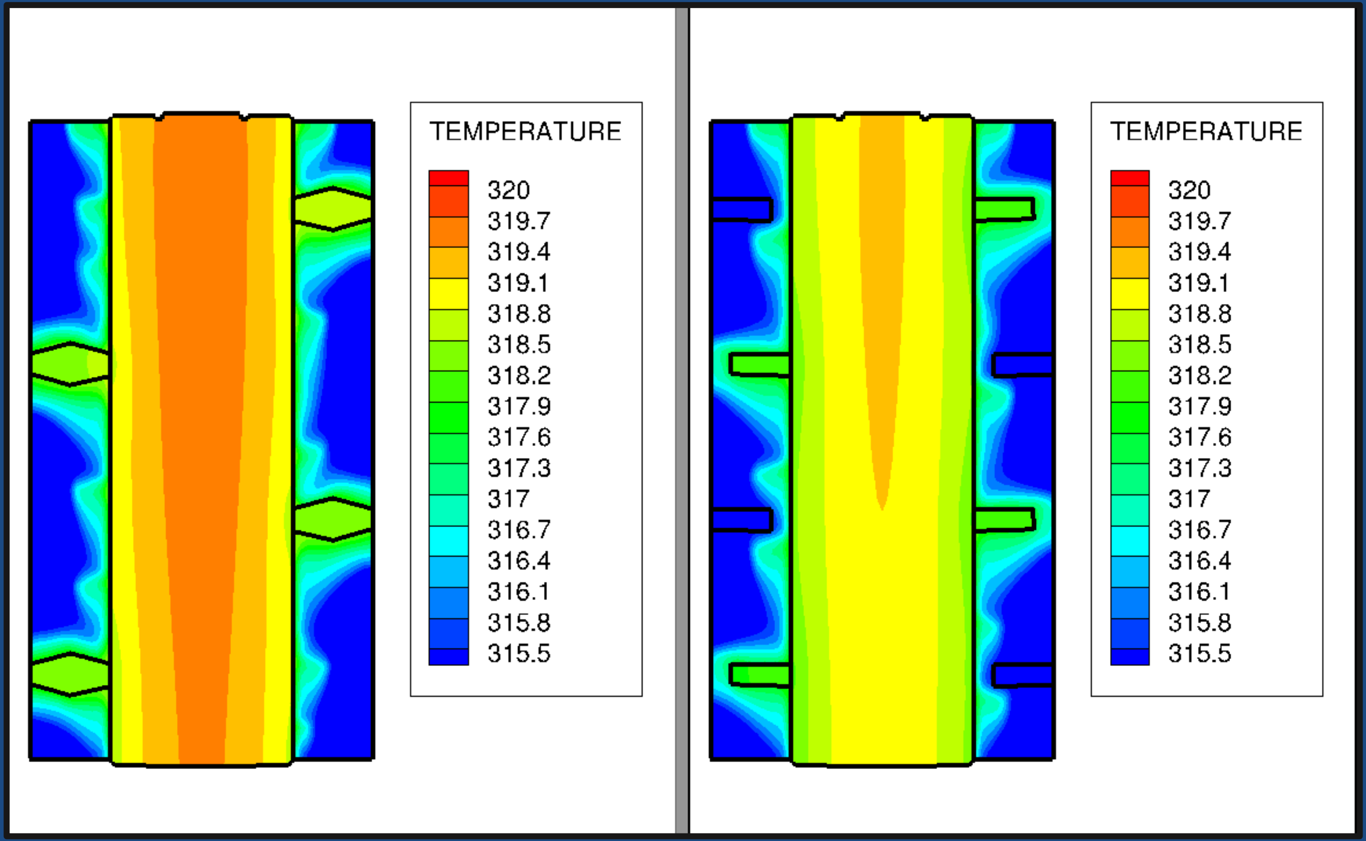

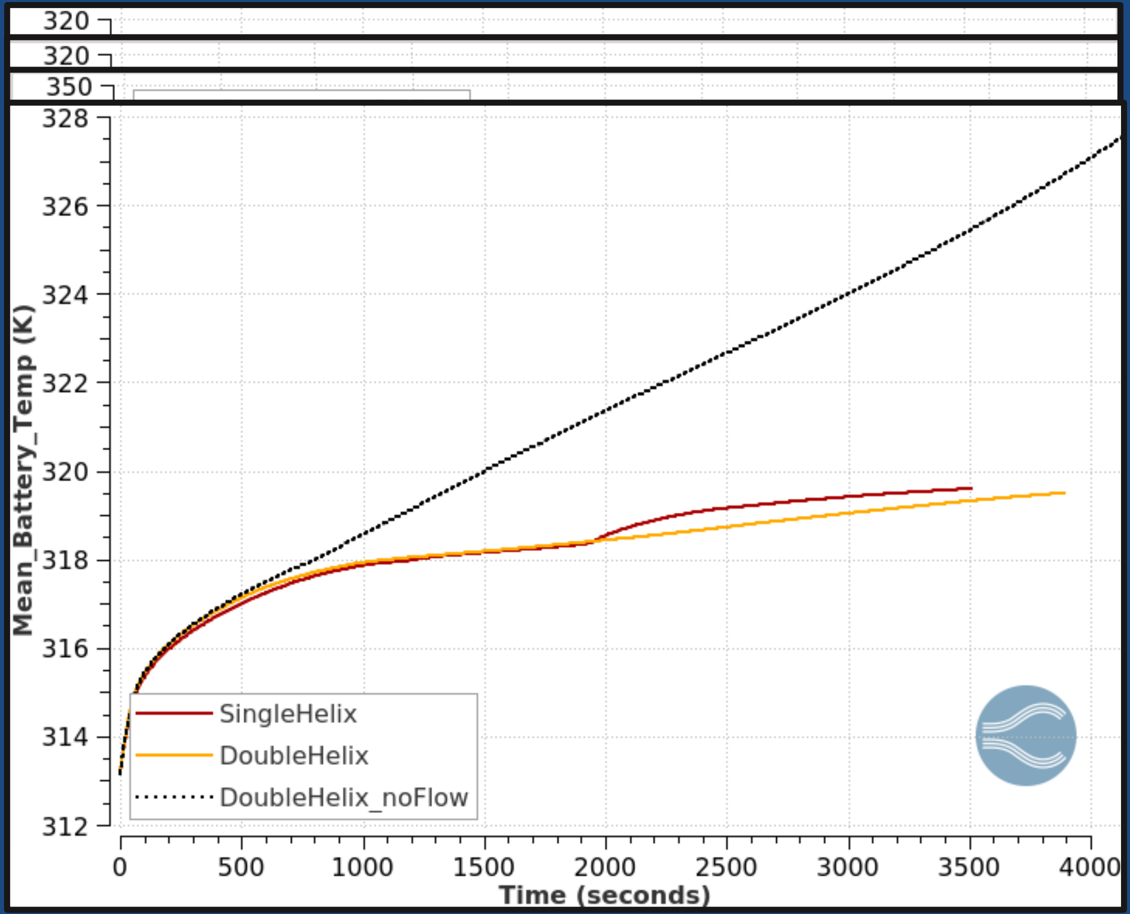

Incorporating 3D Effects : Short-Circuit Model

- Time or Temperature (ISC device) controlled short-circuit event, independent shape/size (for heat release)
- Resistance R_SC : User input

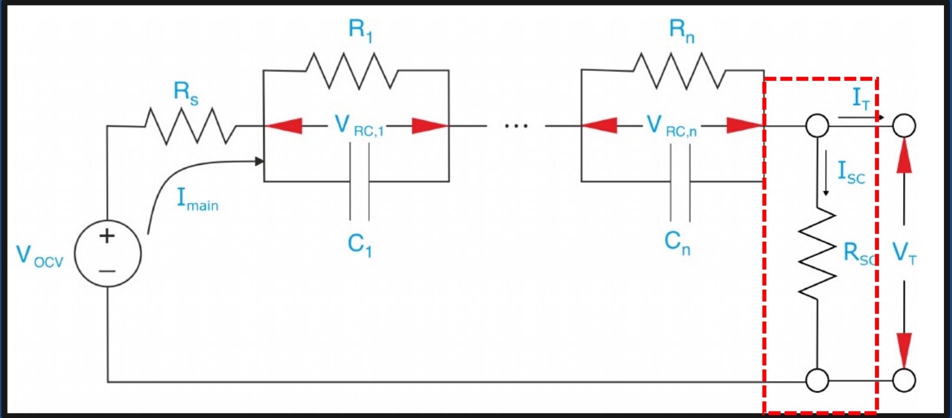

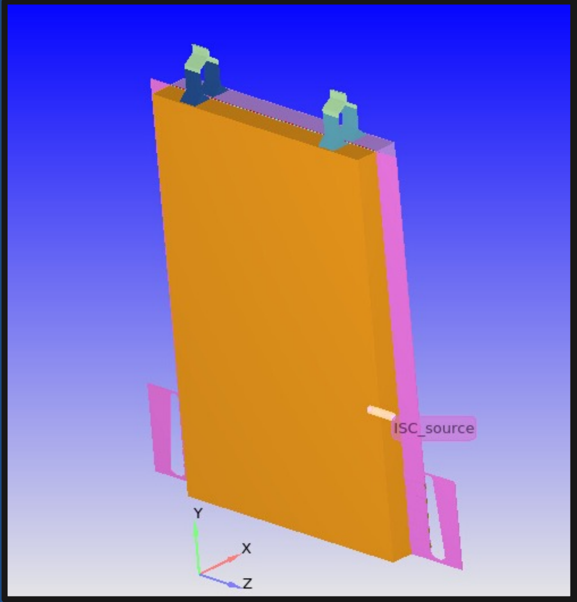

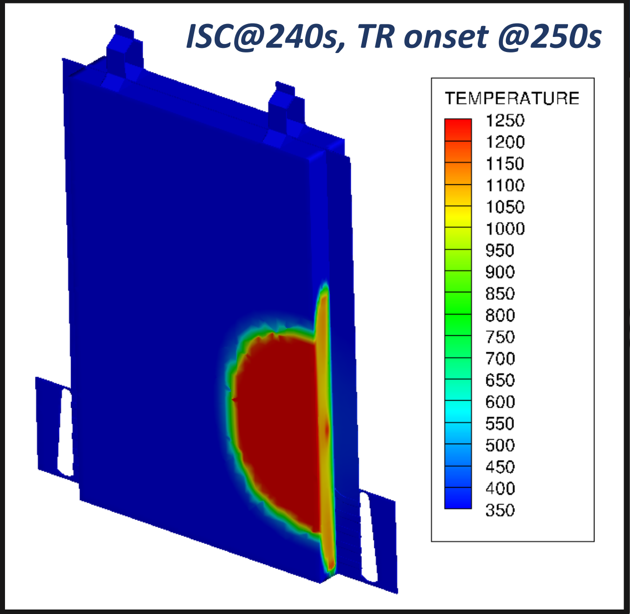

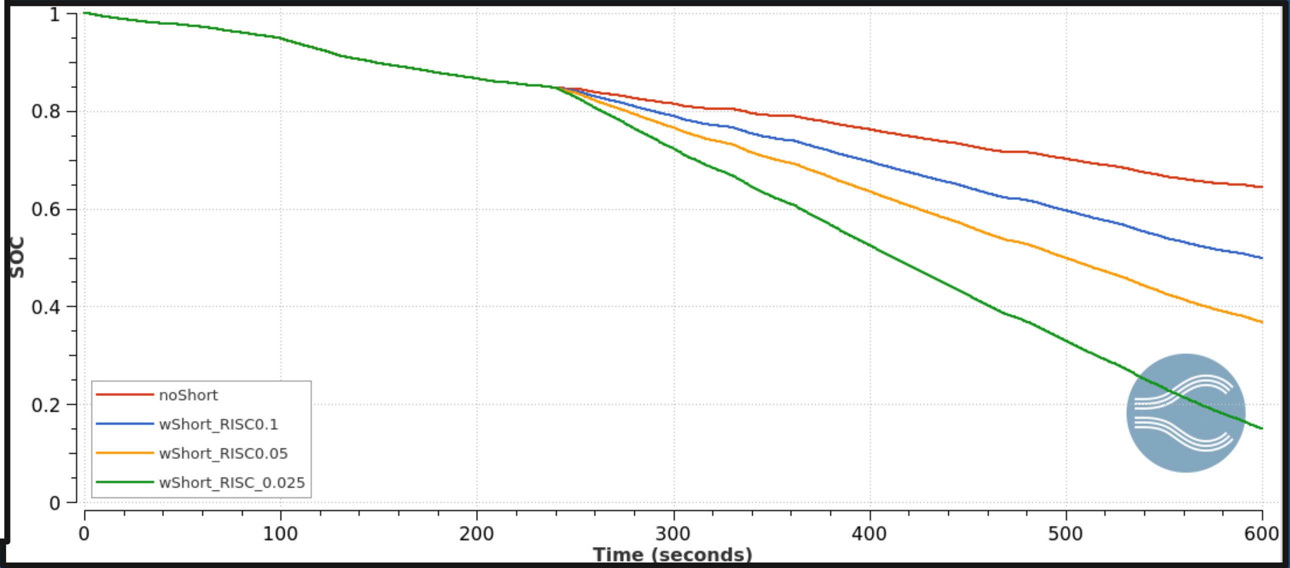

PCM/Fin Assembly Response to Short-Circuit Location

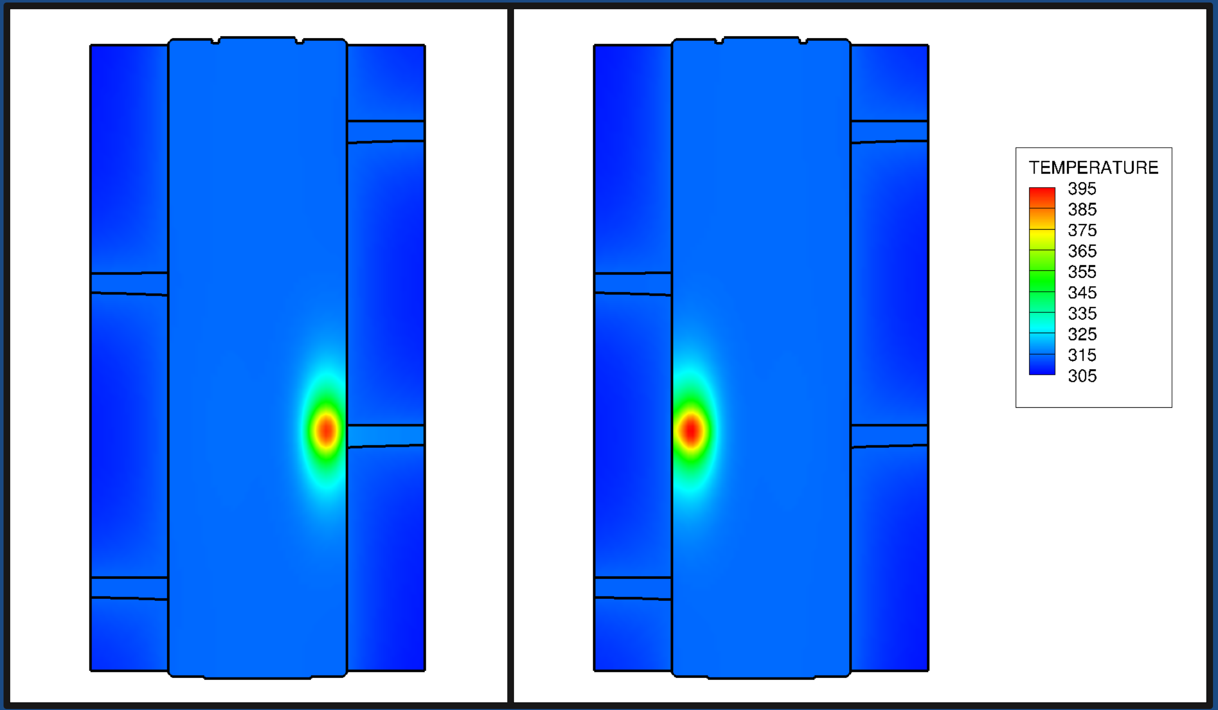

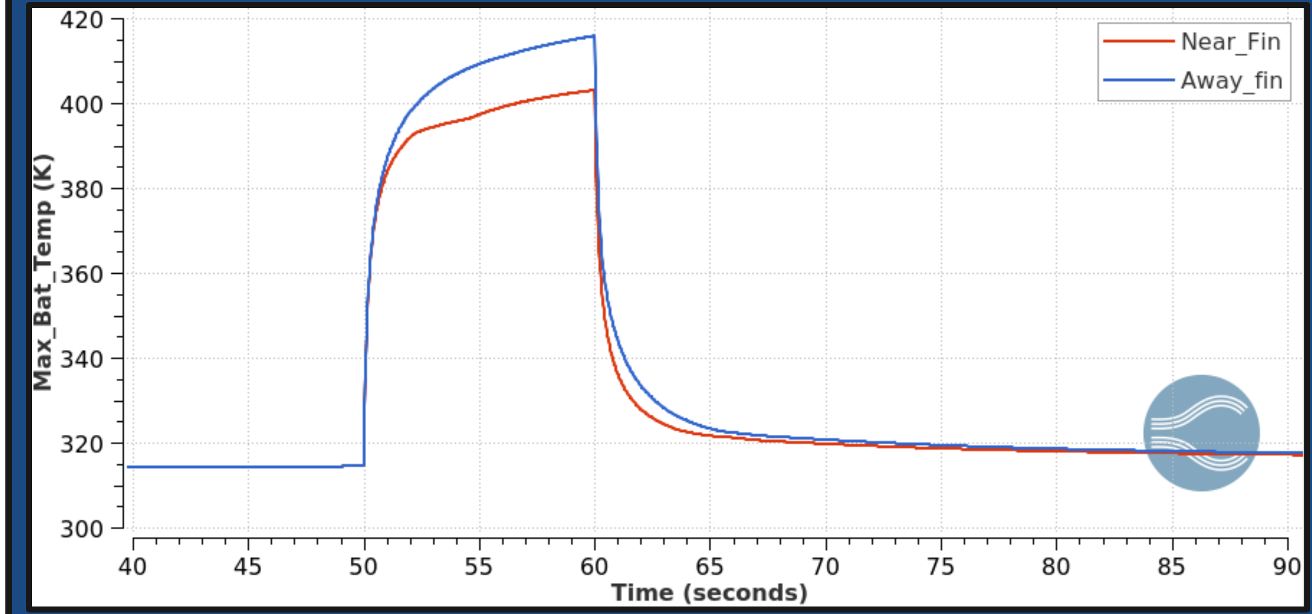

*Thermal runaway model inactive

Non-Uniform Battery Heating

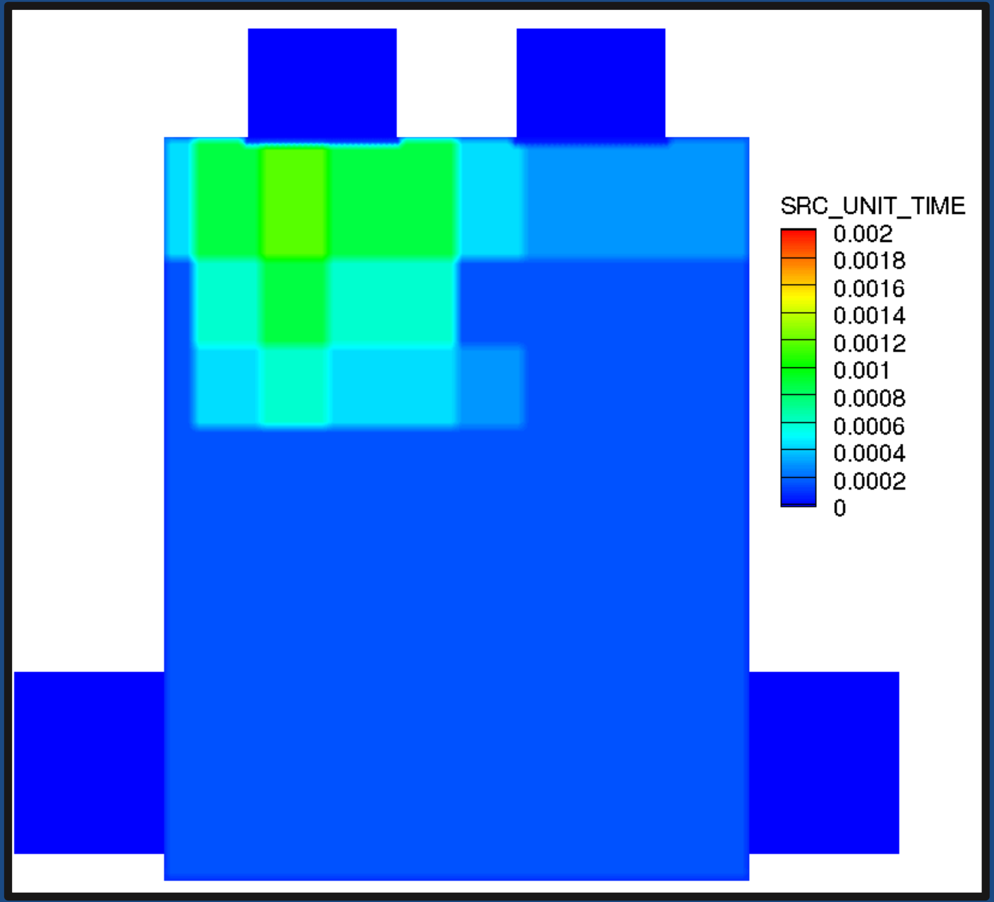

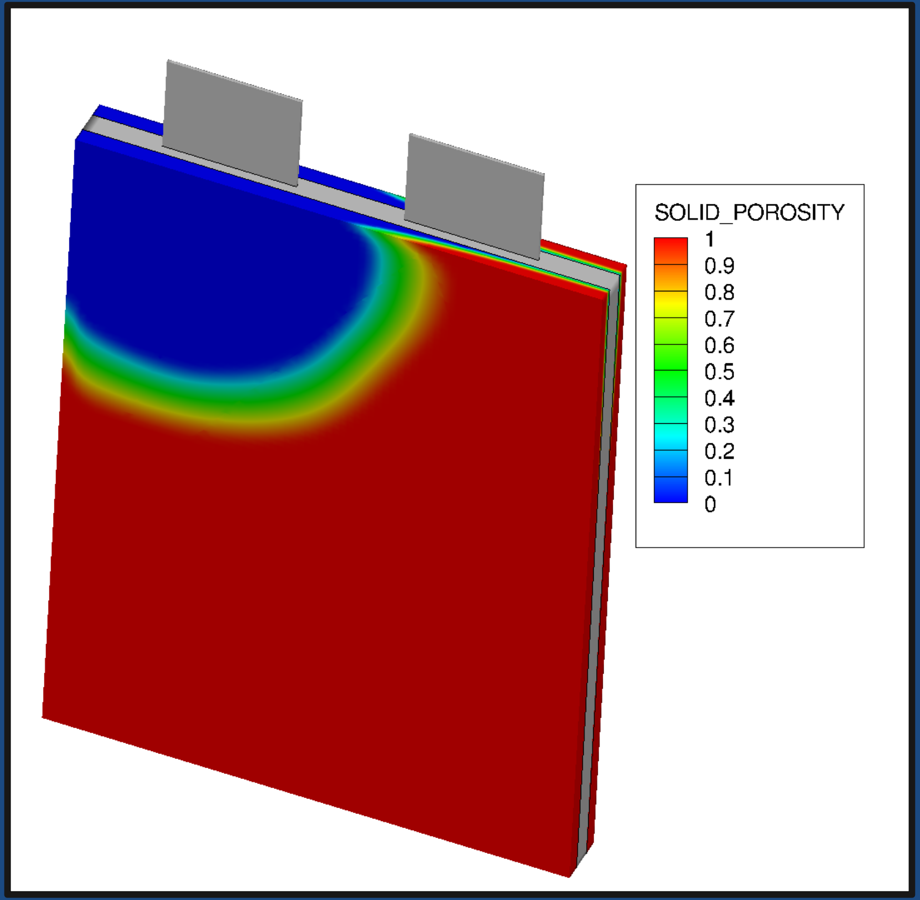

Coupled Electric Potential Solver : A 3D Analysis (1/2)

$$\nabla(\sigma\nabla\phi_1) = S(\phi_1, \phi_2)$$

$$\nabla(\sigma\nabla\phi_2) = -S(\phi_1, \phi_2)$$

$$E_1 = -\nabla\phi_1$$

$$E_2 = -\nabla\phi_2$$

$$Q = \sigma E_1^2 + \sigma E_2^2 + q_{elec}$$

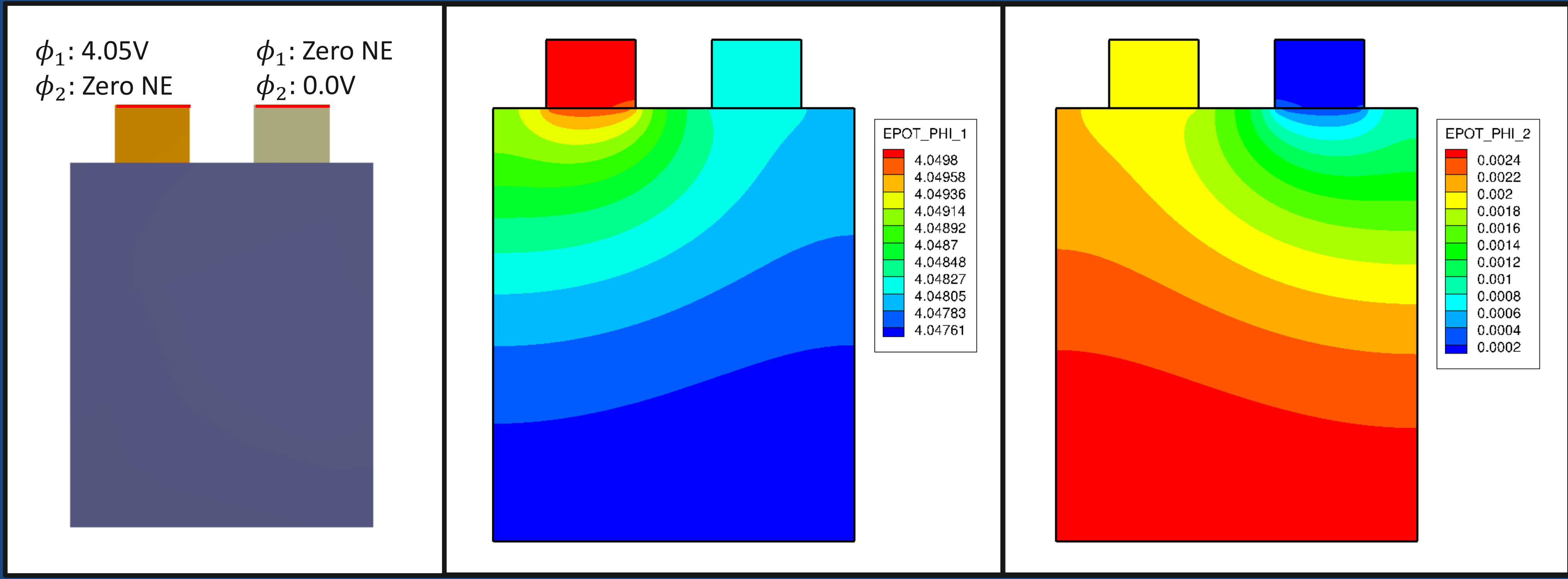

Coupled Electric Potential Solver : A 3D Analysis (2/2)

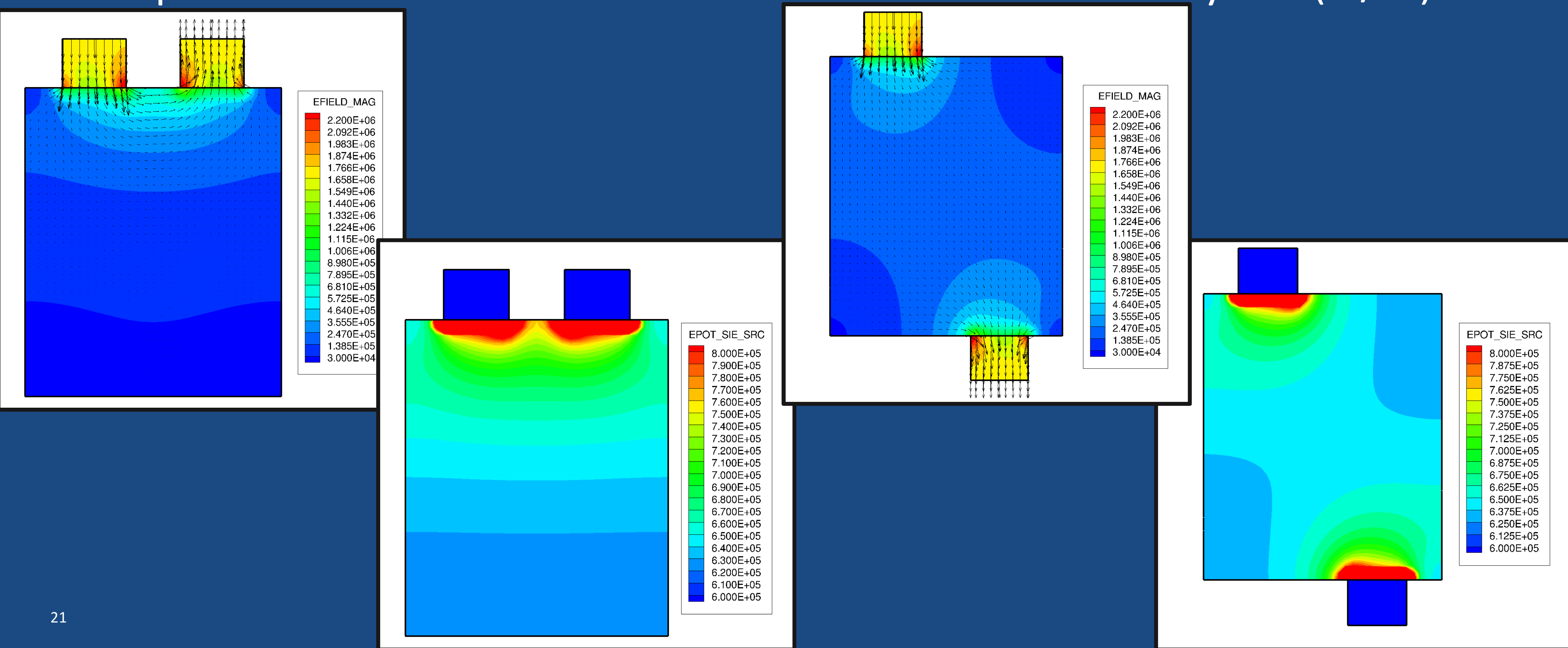

Thermal Runaway Mitigation with PCMs

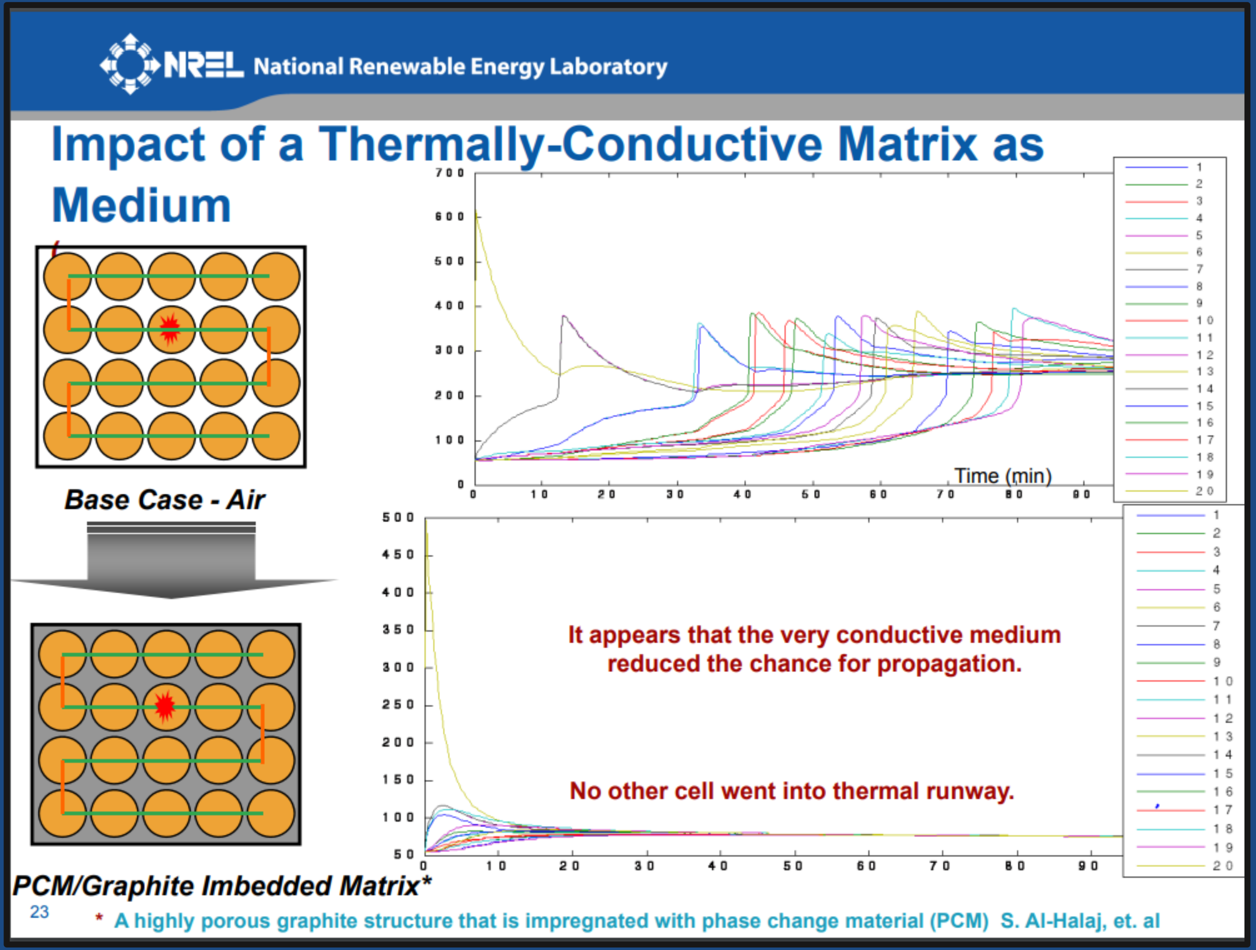

- Impact of "PCM/Graphite matrix on thermal runaway propagation in a module : *G.H. Kim et. al., 212th ECS, Washington, DC, Oct, 2007*
- Thermal runaway reaction model utilized for a predictive analysis
- Are TR simulation results reliable? : Reproducibility and repeatability

Thermal Runaway Propagation Analysis: Chemistry

- Thermal runaway reaction kinetics
  - Hatchard-Kim mechanism : 4 Reactions, LCO battery chemistry

SEI decomposition (sei)

$$R_{sei}(T, c_{sei}) = A_{sei} \exp\left[-\frac{E_{a,sei}}{RT}\right] c_{sei}^{m_{sei}}$$

Anode and electrolyte (ne)

$$R_{ne}(T, c_e, c_{neg}, t_{sei}) = A_{ne} \exp\left[-\frac{t_{sei}}{t_{sei,ref}}\right] c_{neg}^{m_{ne,n}} \exp\left[-\frac{E_{a,ne}}{RT}\right]$$

Cathode and electrolyte (pe)

$$R_{pe}(T, \alpha, c_e) = A_{pe} \alpha^{m_{pe,p1}} (1-\alpha)^{m_{pe,p2}} \exp\left[-\frac{E_{a,pe}}{RT}\right]$$

Electrolyte decomposition (e)

$$R_e(T, c_e) = A_e \exp\left[-\frac{E_{a,e}}{RT}\right] c_e^{m_e}$$

- Calibrated reaction mechanisms required to reproduce experimental behavior
  - Reliant on experimental DSC data

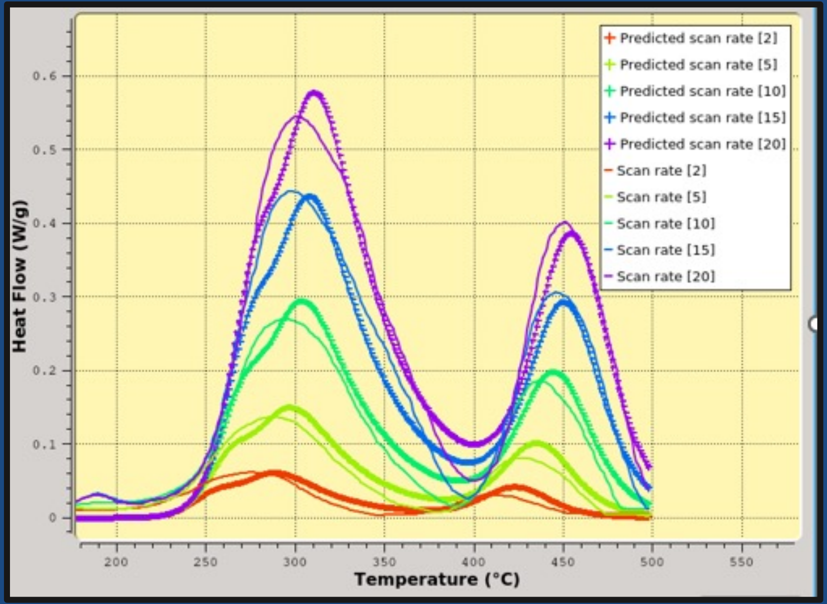

- A comprehensive species-based reaction mechanism for thermal runaway chemistry? : COMPUTATIONAL CHEMISTRY CONSORTIUM

CONVERGENT SCIENCE

Thermal Runaway Propagation Analysis: Statistics

Raw data from the ARC experiment

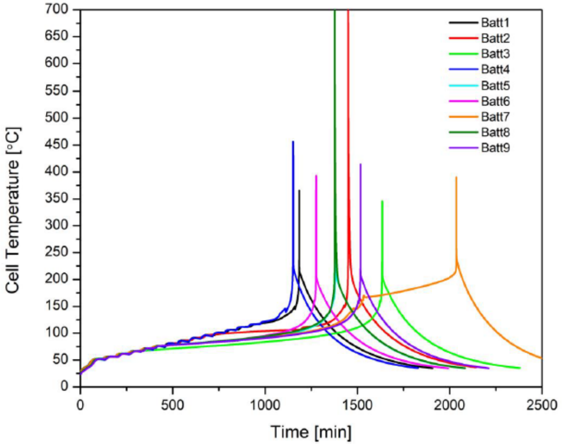

	Exotherm onset Temp[1] T_{exo}(°C)	Thermal runaway onset Temp[2] T_{TR}(°C)	Max Temp[3] T_{max}(°C)	TR delay time (min)
Batt 1	118.17	211.36	365.38	204.33
Batt 2	97.73	210.06	716.45	720.5
Batt 3	67.38	199.98	345.13	1308.96
Batt 4	123.83	220.94	456.48	121.52
Batt 5	77.69	201.14	384.15	897.43
Batt 6	77.44	195.36	392.72	802.80
Batt 7	76.89	228.62	390.33	1584.35
Batt 8	77.54	200.65	726.68	911.74
Batt 9	77.47	204.19	414.42	1044.03

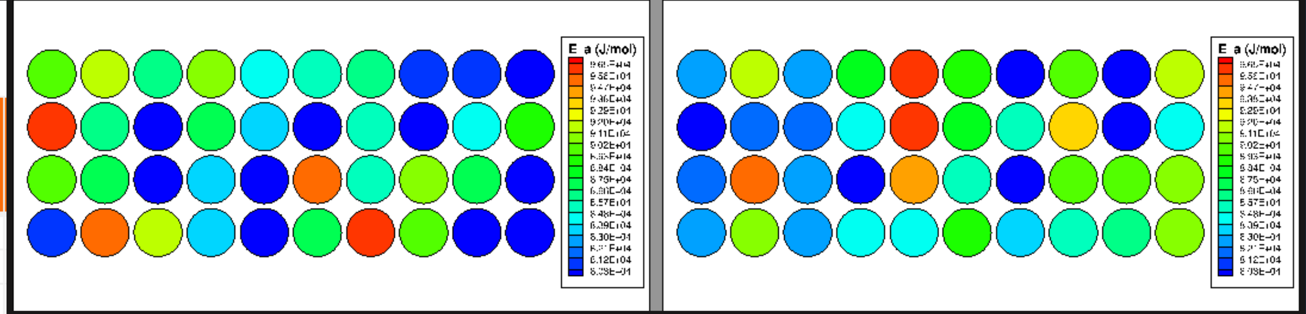

Statistical analysis of frequency factor and global activation energy of all 18650 Samsung LCO cells.

	ΔT_{ad} (K)	c_p (J/kg·K)	H (J/kg)	E (J/mol)	A (min^{-1})
Batt 1	247.2	730	1.80E5	9.65E4	2.00E9
Batt 2	618.7	730	4.52E5	9.33E4	4.10E8
Batt 3	277.8	730	2.03E5	8.30E4	9.00E8
Batt 4	332.6	730	2.43E5	8.39E4	4.50E7
Batt 5	306.5	730	2.24E5	8.03E4	3.77E7
Batt 6	315.3	730	2.30E5	8.33E4	1.06E8
Batt 8	649.1	730	4.74E5	8.24E4	2.99E7
Batt 9	336.9	730	2.46E5	8.36E4	7.40E7
Average	ΔT_{ave}: 385.5	c_{pave}: 730	H_{ave}: 2.29E5	E_{ave}: 8.58E4	A_{ave}: 3.49E8
Standard deviation	ΔT_{SD}: 156.3	c_{pSD}: 0	H_{SD}: 1.73E4	E_{SD}: 5.80E3	A_{SD}: 6.95E8

$$\frac{dc}{dt} = -Ace^{-\frac{E}{RT}}$$

$$c_p\frac{dT}{dt} = HAce^{-\frac{E}{RT}}$$

Zhang et. al. (2022)

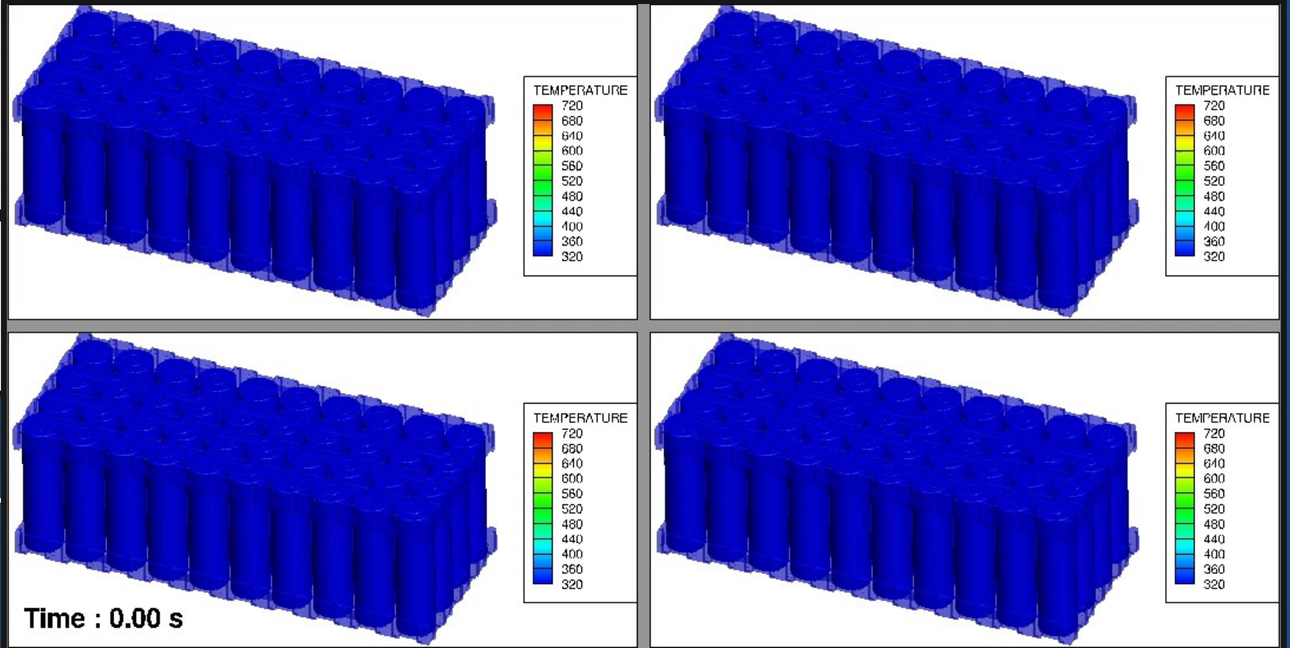

PCMs as Fire Retardants

- Possible use of PCMs as flame retardants
- CONVERGE has established surface chemistry capabilities that can be utilized
- But what ignites the gases?

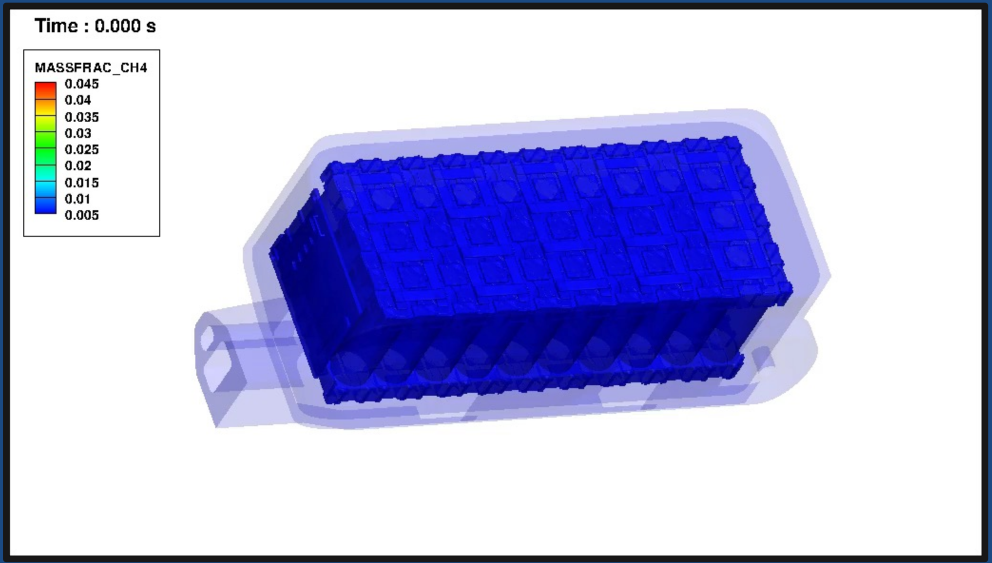

Spark ignited vent gas combustion inside a battery pack

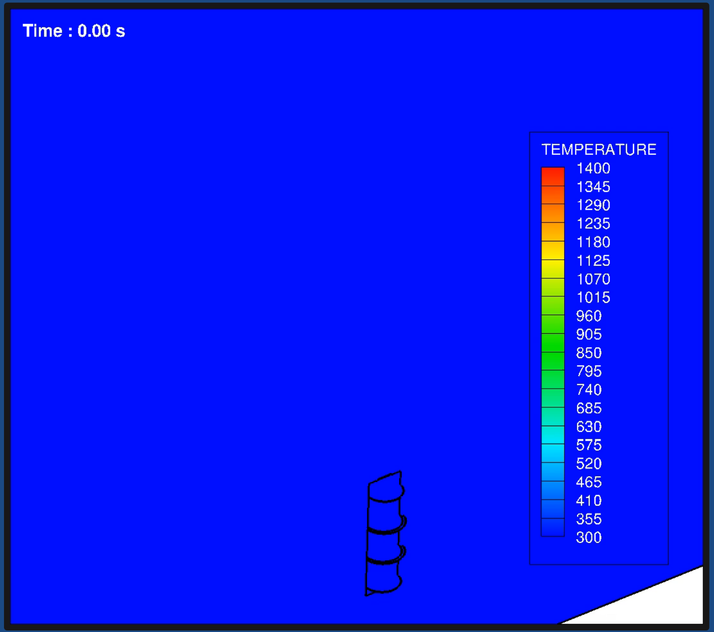

Self ignition of vent gases after exit

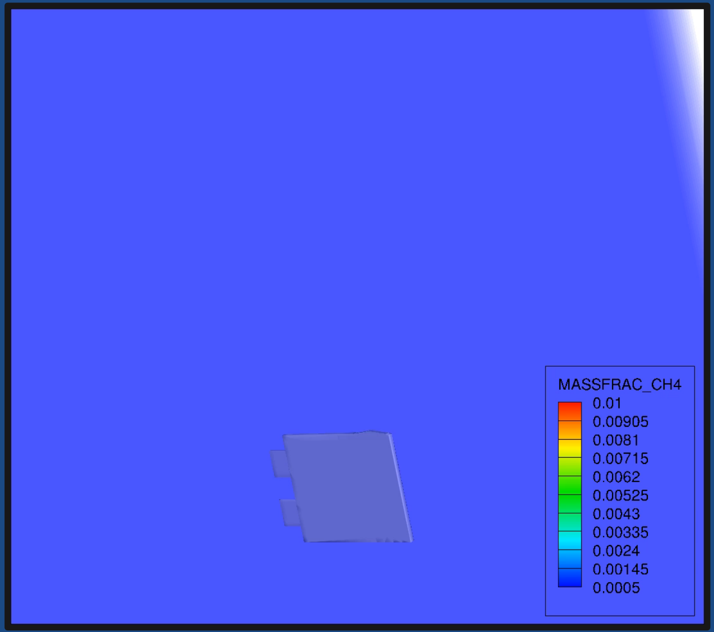

Vent gas ignition due to hot ejecta

Thermal Interactions Between Solid Ejecta and PCM

- Lagrangian solid particle wall film modeling approach for deposition of solid ejecta during thermal runaway and associated heat transfer to walls

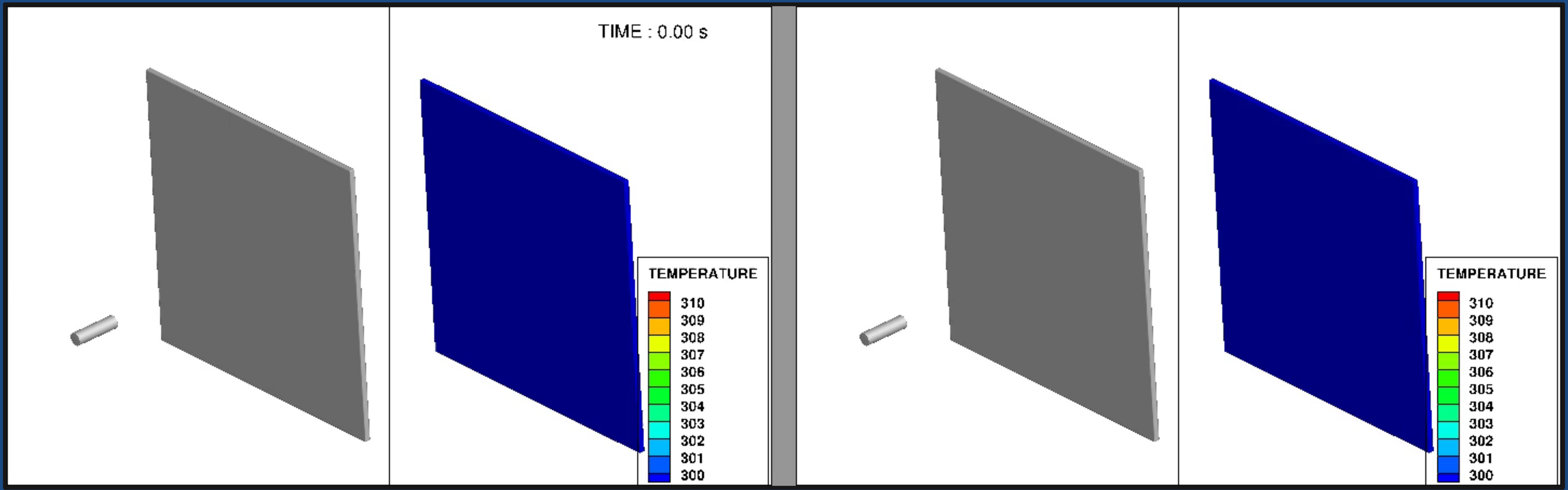

Aluminum plate

Solid with PCM thermal properties

THANK YOU!

CONVERGECFD.COM

Kislaya Srivastava,
Principal Engineer, Convergent Science Inc.
kislaya.srivastava@convergecfd.com

CONVERGENT SCIENCE